Final 371 Project: Static Analysis of a Deflected Endmill

By

ABID BACCHUS, JOHN HUNTER, RYAN CAN, REZWAN ISLAM

City College of New York

Mechanical Engineering

Professor Gary Benenson

ME 37100

Date: 05/30/2017

Table of Contents

Overview

The project focuses on the use of the Finite Element Method (FEM) in engineering analysis. In particular, our project is to analyze the use and function of a flat end mill cutting tool that broke in the manufacturing lab at City College of New York (CCNY). This was not the first tool to break in the manufacturing lab. Every member of our group took the manufacturing class this semester at CCNY, and Ryan Can and Abid Bacchus will be continuing as the laboratory teaching assistants in the Fall semester 2017. Considering the work we had done in this lab and the continuation of the work some members of our group were undertaking, we were interested in why tools were breaking. Our group was in touch with the current technicians in the manufacturing lab, and we began to gather information about the mill that broke with their assistance. With their help, we were able to describe many of the material properties of both the mill we wanted to analyze and the piece of stock that the mill was working(cutting) on. The four-flute flat end mill we studied had a $1/8^{th}$ inch diameter and was made of Tungsten Carbide. The mill was cutting Chromoly steel (alloyed with Chromium and Molybdenum) at a depth of 30 mils when it broke. We proposed, when we had been given the materials, and the cutting parameters, that we could film the tool as it was cutting the workpiece(stock) and obtain the force on the mill by observing the deflection and calculating backwards. If the force was obtained we could then attempt to find the stress distribution in the mill. The geometry of the mill was observable, but the stresses that developed due to the force applied during use were not known. We proposed to use Finite Element Analysis to see where the stress concentrations were most likely to develop, and to see if those stresses matched our predictions and our analytical model. If we could find the location of likely stress concentrations, and if we were able to validate the gathered data with analytical calculations, then we proposed to use the properties of the FEM program(SolidWorks), as a linear solver, to make a recommendation about the depth of cut that the mill could make for this stock piece safely, and without breaking. We were able to make this recommendation after gathering material data, deflection data, converting these data into force and stress predictions based on the depth of cut that the mill could handle. We recommend that this mill not cut this piece of stock at a depth of cut of more 2 mils so that the stress that develops does not exceed the maximum tensile strength of the material.

Introduction

Background and Theory

A flat end mill is a cutting tool that is inserted into an arm on a milling machine or Computer Numerical Control machine so that a piece of stock, or workpiece can be fed to the mill and then shaped by cutting. A milling machine is shown in Figure 1.

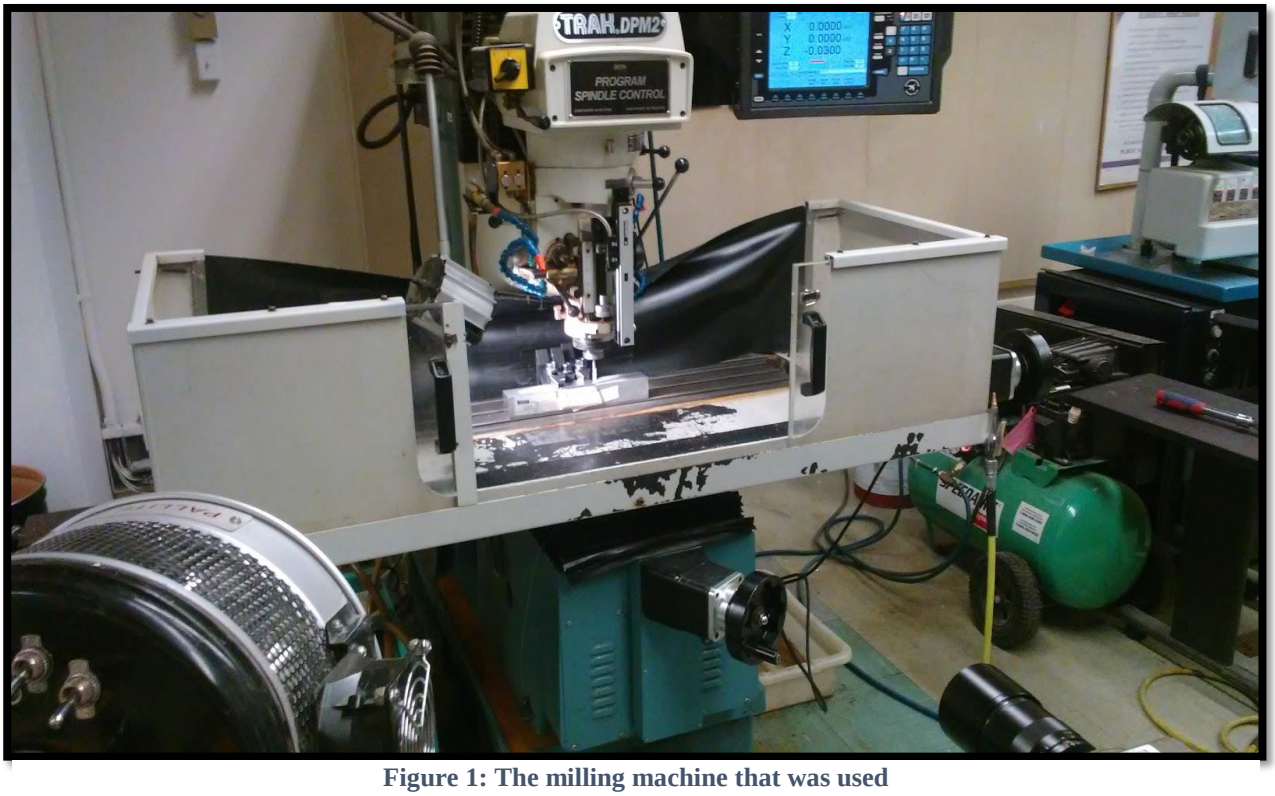

Figure 1: The milling machine that was used

The geometry of the mill is shown in Figure 2. The portion of the tool that comes into contact with the stock is described by the cutting depth. The tool is primarily used for lateral cutting, or cutting with a fix 'z' position, but the stock is able to move in an 'xy' plane orthogonal to the 'z' axis. The stock then can move back and forth relative to the mill, as well as left and right, but does not move up and down when the 'z' position is fixed. The flat end mill does perform plunging operations, where the z position is changed, but does so only while the stock's xy, positions are fixed. The cutting depth created between the stock piece and the mill during lateral cutting is shown in Figure 3.

Figure 2: Shape of mill

The stock piece comes into contact with the mill on the cutting edge of the mill. The movement in the cutting process involves a force on the mill as shown in Figure 3, so that there is some amount of deflection of the tool, however small. It is this deflection, and the stresses that develop along with the deflection, that we think broke the endmill. It is this deflection that we wish to observe and analyze.

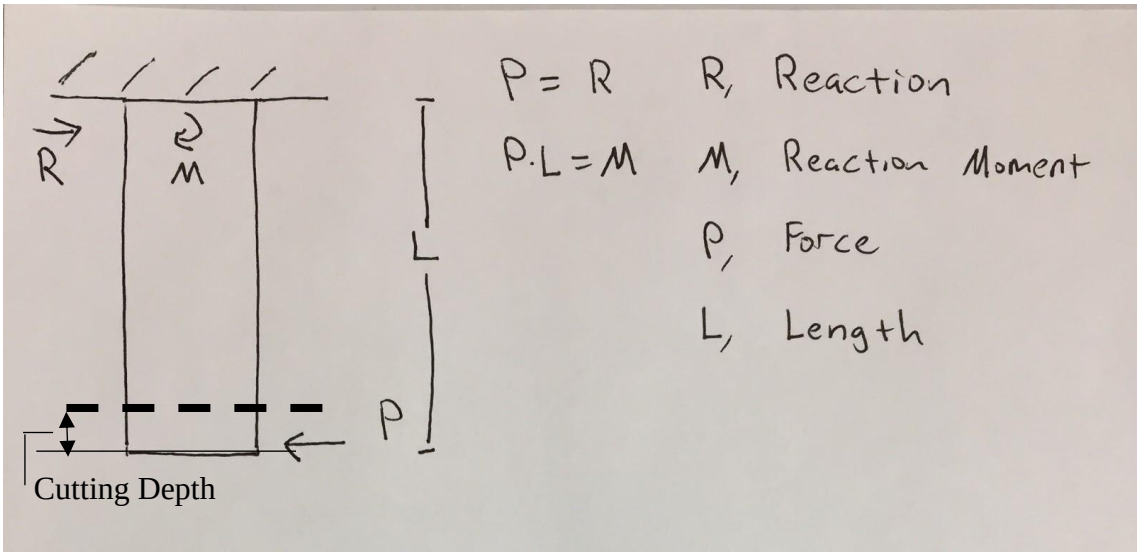

Figure 3: Sketch of system

The mill is inserted into an arm on the milling machine or CNC machine and is held by a fixture called a collet, Figure 4. To begin modeling the situation where the mill broke we show the collet as a fixed end where translation and rotation cannot occur. The fixture of the end mill is shown so that when the force that occurs during movement of the stock a moment is develops about the collet. We then chose to model the mill, and the force applied on it as a cantilever beam.

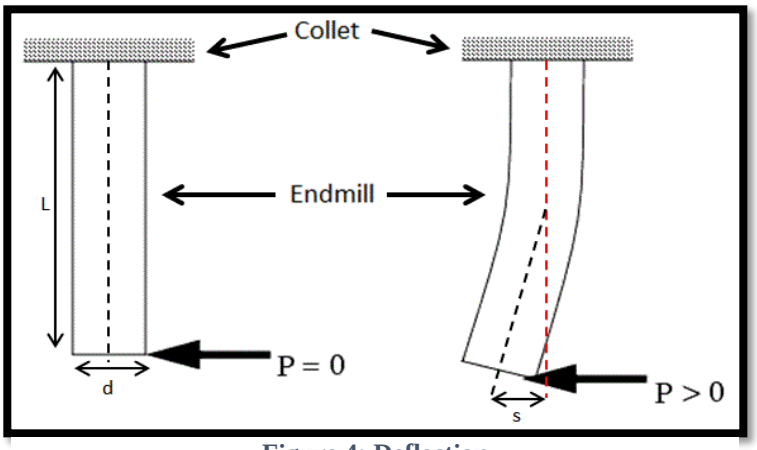

Figure 4: Deflection

The geometry used in most cantilever approximations is generally simple. Rectangular or circular cross-sections are used most often to analyze systems if the approximation can be justified. Our mill is roughly circular, but there are many changes in geometry along the flute length which contains the cutting edge as shown in Figure 5.

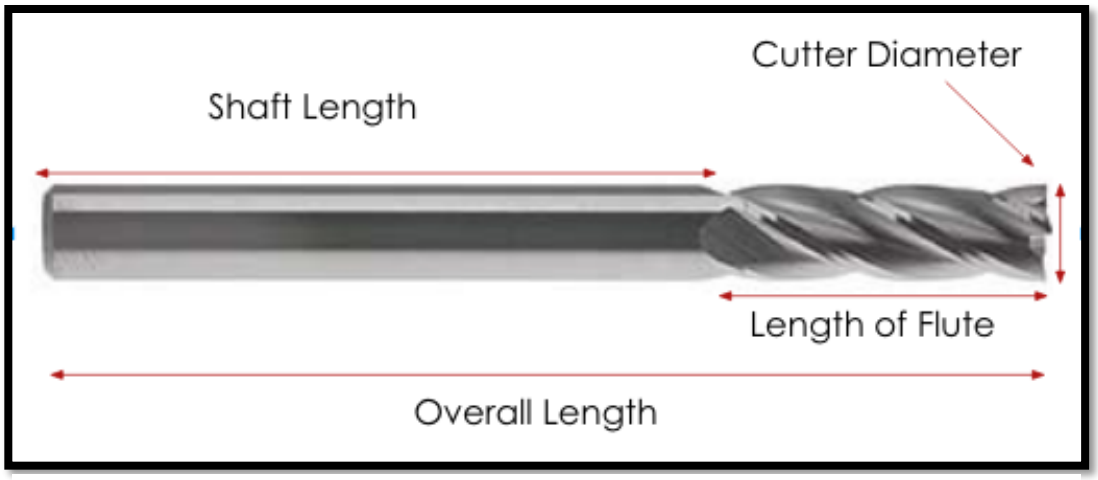

Figure 5: Basic components of an endmill

Due to the changes in geometry we created a model that is not as simple as a circular cross-sectional model, but is closer to the geometry of the mill that was used.

Milling tools break, and investigations into the reasons behind the failure of these tool have been done in the past by other groups. One group that has performed extensive studies on the failure of end mills similar to ours is the American Society of Mechanical Engineers (ASME). In a paper presented at the 2003 ASME International Mechanical Engineering Congress & Exposition, Evren Kivanc and Erhan Budak show the development of a static analytical model that describes the deflection and stresses in four flute end mills similar to the one being analyzed in our project. The paper by Dr. Kivanc and Dr. Budak describes the deflection in end mills by modeling the tools as cantilevered beams. The static analysis they describe in the paper uses experimental data to develop relationships, described by equations, between the tool's geometry, the force applied to the tool, and deflection that will occur due to the application of force.

In the paper, "Development of Analytical Endmill Deflection and Dynamic Models", Dr. Budak and Dr. Kivanc begin with a cantilever beam model, and through experimental data develop and confirm a more precise mathematical relationship between the force incident on an end mill and the deflection that occurs as a result of the force. The model they develop takes into

account the geometry of the cutting edges and the circular portions of the shaft, to improve upon a simple circular cross-section cantilever model. Here we will look at this model which we think is a better approximation of the end mill we analyzed than a simple cantilever beam model that does not take into account the changes in geometry around the flutes.

Analysis of Tool Geometry

Figure 6 shows the component features of the end mill, where D1 is the flute diameter, D2 is the shaft diameter, L1 is the flute length, L2 is the overall length, I1 describes the area moment of inertia in the shaft, and I2 describes the area moment of inertia in the flute length. The force incident on the mill is called F in the model, Figure 6. Budak and Kivanc use moment-area theorems to develop the equation that gives the maximum deflection, δmax, of the end mill as follows:

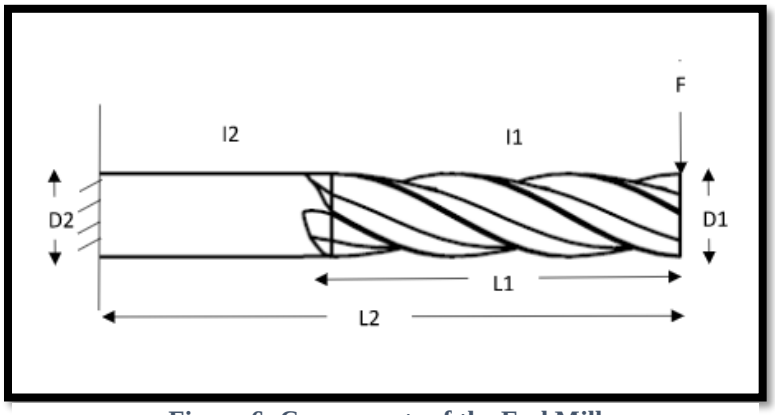

Figure 6: Components of the End Mill

$$\delta_{max} = \frac{Pl_1^3}{3EI_1} + \frac{1}{6}\frac{Pl_1(l_2 - l_1)(l_2 + 2l_1)}{EI_2} + \frac{1}{6}\frac{Pl_2(l_2 - l_1)(2l_2 + l_1)}{EI_2} \qquad \text{Maximum Deflection}$$

$$P = \frac{\delta_{max}}{\left[\frac{l_1^3}{3EI_1} + \frac{l_1(l_2 - l_1)(l_2 + 2l_1)}{6EI_2} + \frac{l_2(l_2 - l_1)(2l_2 + l_1)}{6EI_2}\right]} \qquad \text{Applied Force}$$

Several material and geometric properties are needed to solve for the maximum deflection. The area moments of inertia need to be calculated separately, while the lengths and diameters come from actual tool that we have in our possession. The material property E, the young's modulus, or elastic modulus, is specific to the material the mill is made from. In our case the material is Tungsten Carbide, which has a young's modulus of approximately 675 GPa.

This value is taken from MatWeb. In the analytical modeling, we performed in our project, these values needed to be carefully considered; their values needed to be the same as the values we would use later in our FEM analysis.

Tungsten Carbide is a material made from Tungsten and Carbon in roughly equal parts by number of atoms. The bonds that hold it together are of a metal, Tungsten, and a non-metal, Carbon. Tungsten Carbide, often referred to simply as Carbide, is generally classified as a ceramic material due to the presence of a metal and a nonmetal bonded. Ceramic materials can often have high values for hardness, but do not perform well in tension due to their brittle nature. When brittle materials fail they often do so according to Rankine failure criterion which "Assumes failure will occur when the maximum principal stress at any point reaches a value equal to the tensile stress in a simple tension specimen at failure." This means that when we are using our mill, and we don't want it to break, then we want to keep our maximum principal stress under the ultimate tensile strength of Tungsten Carbide, which is approximately 350 MPa, a value also taken from MatWeb.

In order to keep the maximum principal stress under the ultimate tensile strength we need to understand the stress distribution throughout the end mill. The stress distribution describes the locations of maximum stress as the load is applied to the tool. A moment will develop about the fixture in the model, and the collet in the actual mill. The bending moment that develops there will produce stresses from bending that are higher than anywhere else in the object. But the locations of stress concentrations are harder to predict. We do see changes in geometry where stress concentrations are likely, but because we can only estimate the load paths, we can only estimate the locations of stress concentrations.

Need for FEM

In order to get a better idea about the stress distribution in the tool, the locations of stress concentrations, and to be able to provide some cross validation between the analytical model and an FEA model, we propose to analyze the flat end mill using the Finite Element Method.

Problem Statement

When defining the nature of the specific project that our group did, we had to look at what we knew, and what we did not. We had been in touch with the machinists who worked in the shop where the cutting tools were breaking, so that, when a tool would break, we knew what materials the tools were made of, and the conditions under which the tools were breaking, i.e. the depth of the cut the tool was making, the speed the tools were spinning, the feed rate that the bed on which the stock was secured was moving toward the tool, and most importantly we were able to look at the fracture surface of some of the broken tools. The fracture surfaces were observed to be smooth (shown later in Figure 14), along with the lack of observable yielding and in conjunction with knowing that the flat end mill is a very hard ceramic led us to think that the failure of the Tungsten Carbide tool which we are analyzing was brittle failure.

However, we did not know what the stress distribution was in the tool when it broke. We also did not understand why the force that was applied was sufficient to have the stress develop at high enough values to cause failure. Our problem then is this: *how do we find the stress distribution throughout the endmill and how it varies with the depth of cut, so that we are able to make a recommendation about the use of the tool so that the maximum principal stress stays below the ultimate tensile strength of Carbide.*

Our proposal is to use the known properties of the materials, along with the conditions under which the tool was being used, develop a data gathering process so that we can approximate the forces and stresses involved when the tool failed, and use both FEA and an analytical result to cross-validate our models so that we are able to make a recommendation about the depth of cut so that the maximum principal stress is below the ultimate tensile strength during operation of the flat end mill on the stock piece it was cutting.

Methods

Video Data and Deflection Acquisition

Approximating the forces was a necessary step in making any recommendation. Without approximating the force, we could not approximate the stresses that were involved in the failure of the flat end mill. We looked into setting up a high-speed video camera to observe the deflection of the tool in use. We chose to use a mill of a type very similar to the mills that had been breaking in the lab previously. Additionally, we used the same stock that had was being cut when the last end mill that broke failed. We thought that if during use, the stock applied a force on the mill then the mill would deflect. If we were to observe that deflection then we could approximate the force. As closely as we could, we recreated the situation under which the previous mill broke.

We set up a high-speed camera with the aid of Ken Gollins, the teaching assistant for this course ME 371, so that we could observe the milling process at 9000 frames per second. We thought that the frame rate would allow us to observe the deflection in sufficient detail to calculate the force involved based on the deflection with reasonable confidence. The camera we

Figure 7: High Speed Camera

used is pictured in figure 7. The Ametek Phantom v710 is capable of taking 1.4 million frames per second, but we did not think we needed that kind of frame rate to observe the deflection.

Figure 8 Stock being cut

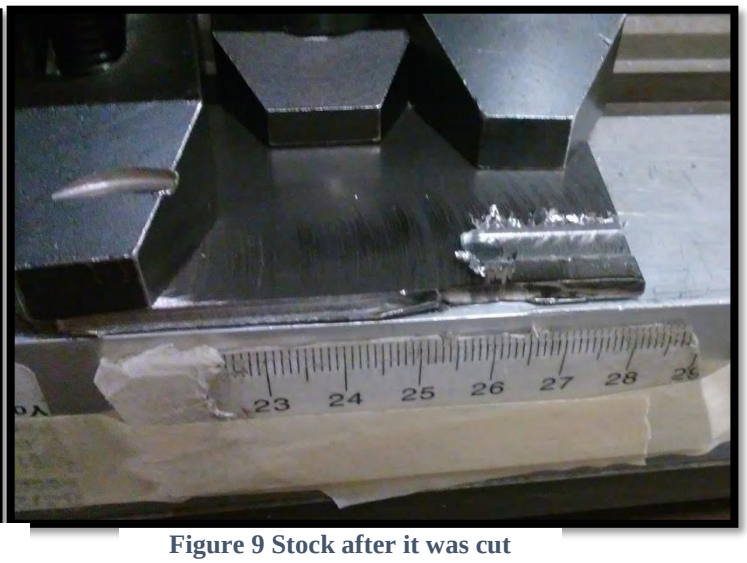

Figure 9 Stock after it was cut

When watching the video from the beginning to the point right before the end mill broke we noticed that the deflection increased as the video progressed. We also noticed that the direction of deflection did not seem to change. As the tool rotated the curvature that developed in the tool relative to the viewing angle only changed in magnitude and not in direction. At any one still frames in the video we were observing a force acting on a more or less cylindrical beam that was fixed at one end so that a deflection occurred. If the deflection direction had changed we may have been dealing with more vibrational effects and a static study may not have been a useful study to do. Because there were many still frames we could observe and that each of them showed a situation that was easily modeled in a static study, we considered SolidWorks simulation to be a valid tool to analyze this situation.

We watched the video so that we knew when the tool broke. We assumed that the force that caused the stresses which broke the end mill were at a maximum at the moment before the tool broke and that they produced the largest deflection, we took a screen shot from the video just before fracture occurred. Figure 11 is a shot taken at time 56 sec from the video and a shot from time 57 sec.

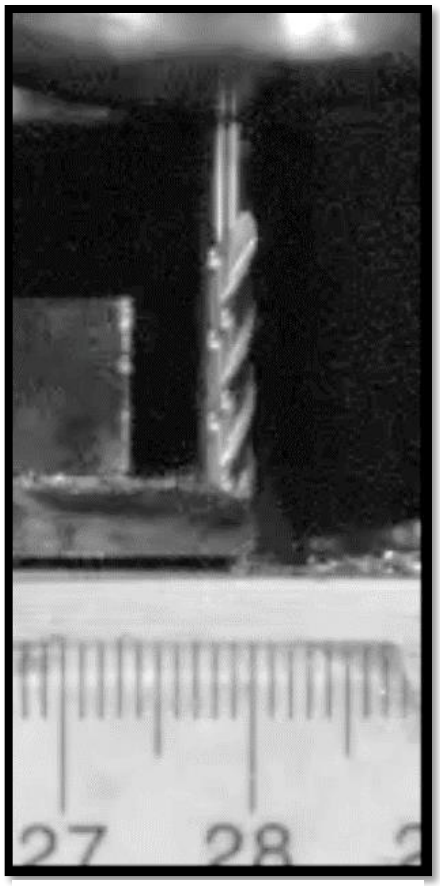

Figure 10 Still shot at start of video with minimal deflection

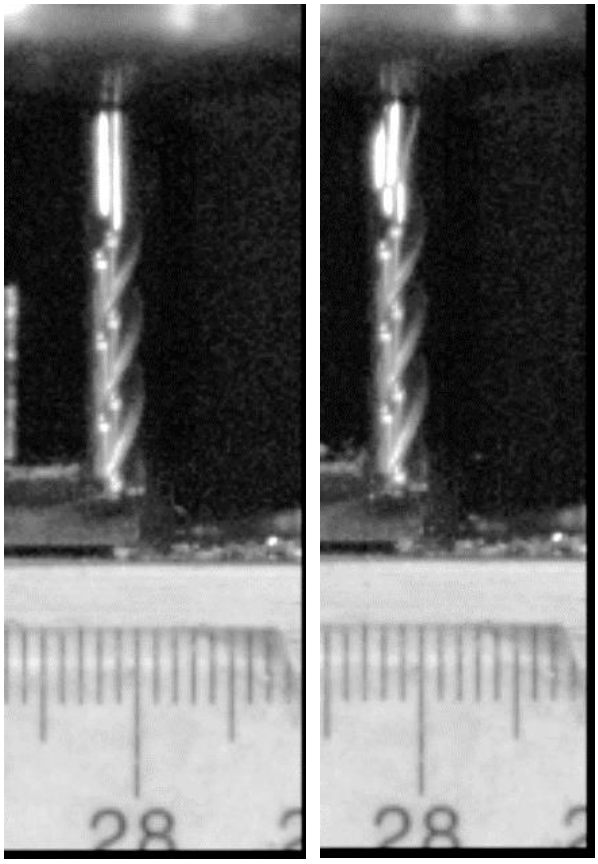

Figure 11 (a) Still shot right before breakage. (b)56 sec on left, 57 sec on right

The snapshot of the video, Figure 11a, was taken the moment before the fracture occurred, so that the image could be used to measure the maximum deflection of the endmill before failure. The image was imported to SolidWorks so that the measurement could be made. The size of the image was scaled appropriately by lining up 5mm of the ruler in the image with a 5mm line sketched in SolidWorks. A 3.17mm (1/8th inch) line was sketched with two lines extending perpendicularly from its endpoints, this was used to represent the non-deflected end mill, and the 3.17mm line was placed where the endmill meets the collet. Another (center)-line was then sketched, parallel to the axis of the endmill, to where the tip of the endmill shows maximum deflection, circled in red in Figure 12 (on next page). The distance between the lines corresponding with the non-deflected end mill and the deflected endmill were measured using SolidWorks evaluation tools. The maximum deflection was measured and taken to be 0.59mm.

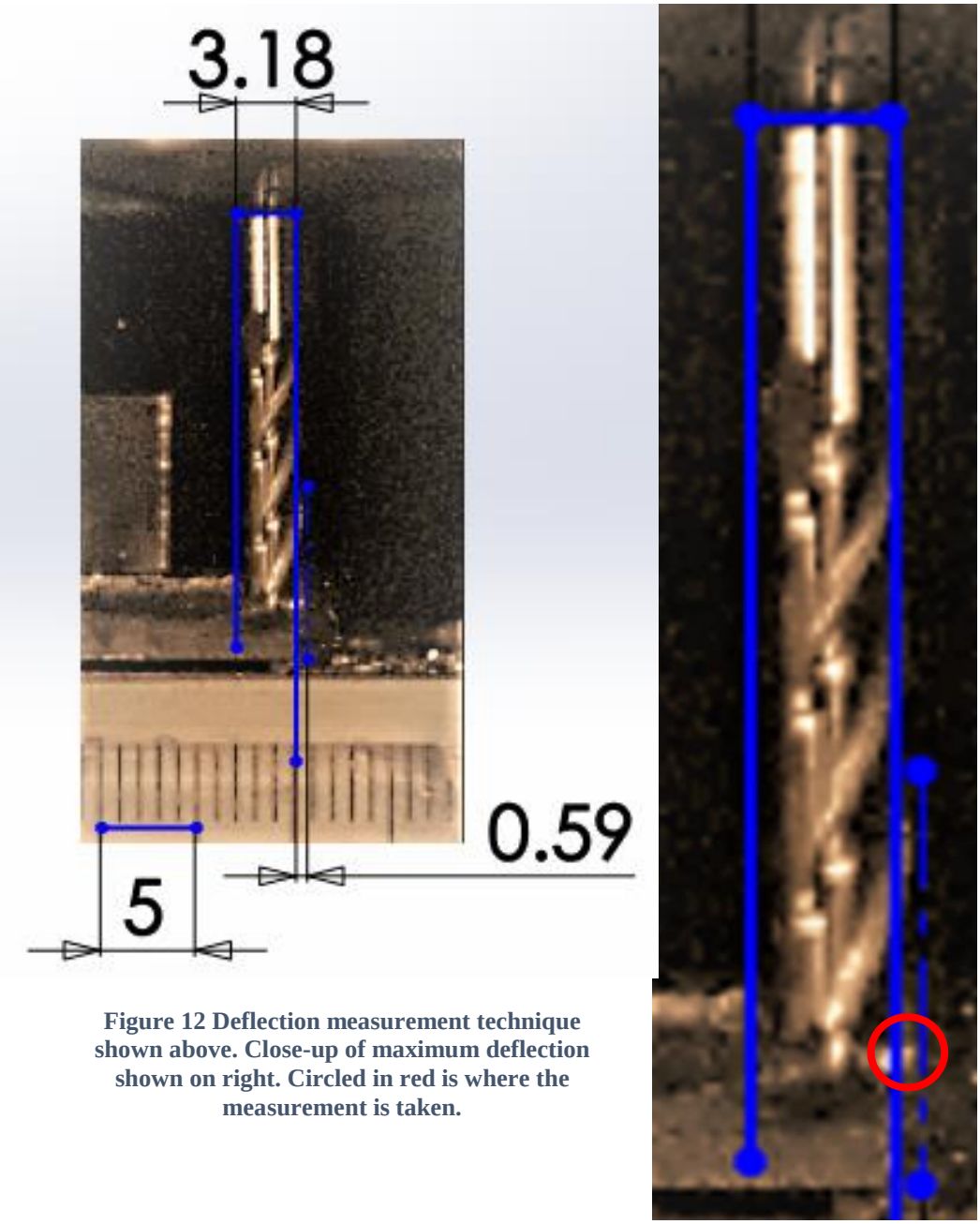

Figure 12 Deflection measurement technique shown above. Close-up of maximum deflection shown on right. Circled in red is where the measurement is taken.

Predictions and Failure Theory

From the video, and from watching it happen live, we knew that the mill had broken during use. Having sketched the part, and described the forces, we surmised that a bending moment had developed about the collet. We also knew that there were changes in geometry in the flute length where stress concentrations that we could not really predict might occur. We thought that it was most likely that either the bending stress near the collet (1), or a stress concentration somewhere in the flute length (2) that caused the failure of the tool, Figure 13.

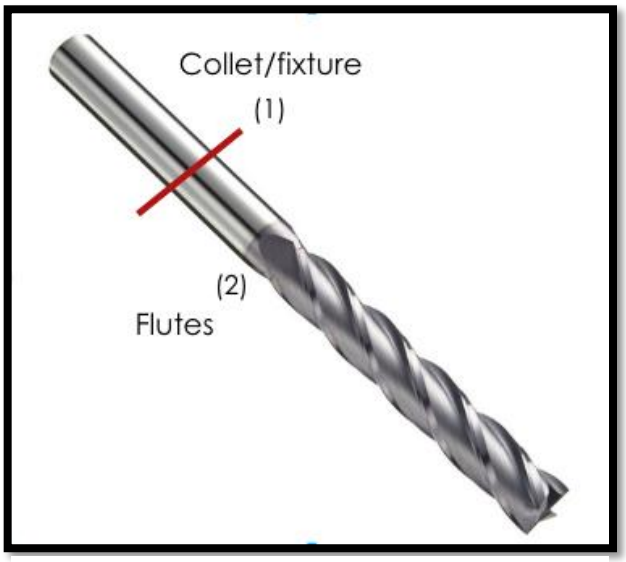

Figure 13 Predictions

Knowing that the fracture surface was smooth, as shown in Figure 14, and that the material the end mill is made from, Tungsten Carbide, is a ceramic, and ceramics generally fail due to brittle failure, we applied the Rankine Failure Criterion which "assumes brittle failure will occur when the maximum principal stress at any point reach a value equal to the ultimate tensile strength of a simple tension specimen at failure." That is, we believe that a stress developed in the end mill that exceeded the ultimate tensile strength of Tungsten Carbide, 350 MPa approximately. But we did not know if this occurred at the collet fixture or possibly at a stress concentration area somewhere in the flute length. In order to find the location of this stress concentration we employed FEA.

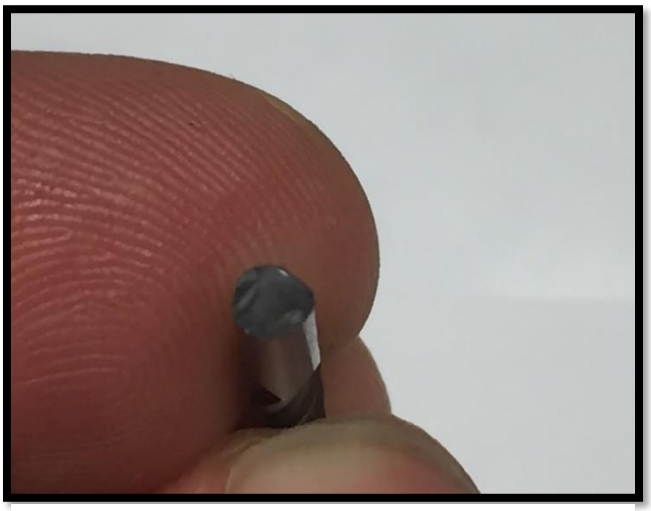

Figure 14 Fracture Surface

Basic Sketch of Model

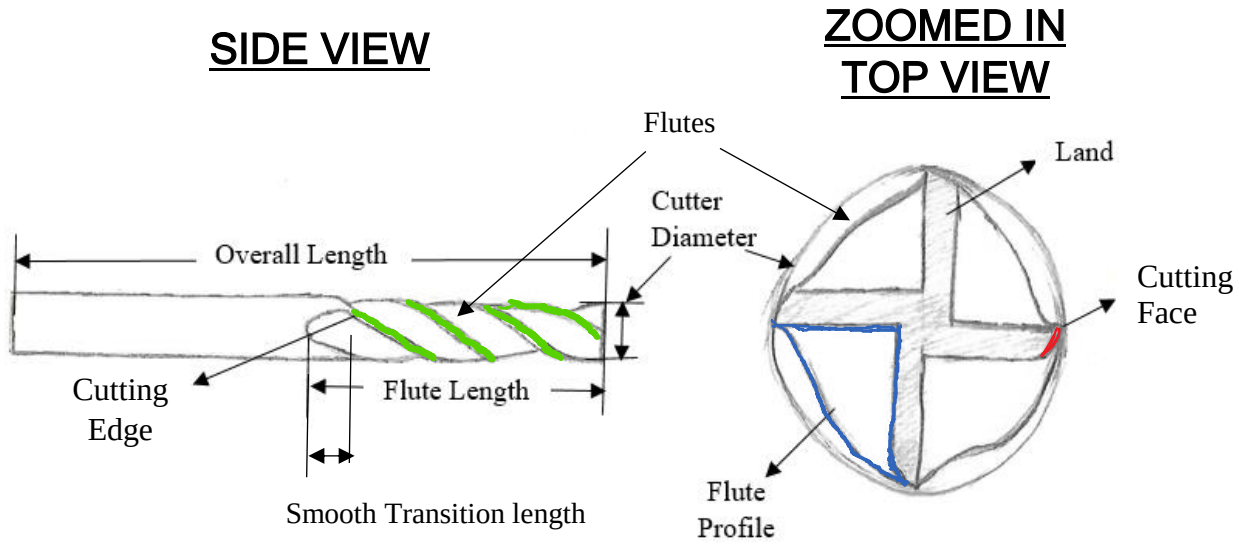

Figure 105 Free Hand Sketch with major components labeled.

A free hand drawing of the flat end mill is shown above with its major components labeled. The figure shows two distinct views of the end mill, a side view and a zoomed in top view. From the side view we can see that the end mill has 4 major parts, the overall length, the flute length, the cutter diameter, and the cutting edge. The overall length, as the name implies, is the total length of the flat end mill. The flute length represents the length of the end mill where the flutes are. The smooth transition length, as seen in Figure 15, will be discussed later on in further details. The cutting edge represents the edge that is used for lateral cuts (green in figure 15). The cutting diameter is the diameter of the end mill. In the top view, we can see that the end mill consists of the four teeth, the flute profile and the land. The land is the flat portion of the face. The cutting face (marked in red) is the starting position of the cutting edge which follows along the flutes (green in figure 15). These names of the major components will be mentioned

throughout the solid modeling procedure. Below is a general overview for the solid modeling procedure.

- Cylinder Extrusion
- Sweep Cut
- Circular Pattern
- Smooth Transition Cut
- Circular Pattern 2

Solid Modeling Procedure

In this section, we will be explaining how the major measurements for the 1/8th inch end mill were made and how they were utilized to create the solid model on SolidWorks. One of the main characteristics of any kind of mill are its flutes. The flutes are the ridges of an endmill and they are defined by their helical shapes. A helix is a spiral structure that contains a repeating pattern and will be discussed later on in further details. So, our first task was to figure out how to produce those flutes on SolidWorks. After some close inspection, we realized that the 1/8th inch end mill is basically a cylinder if the flutes and other details were taken away. That gave us the idea that we should begin our solid modeling process from a basic cylinder.

To make a cylinder in SolidWorks, only two pieces of information are required which are the diameter of the cylinder and the total length to be extruded. By using a caliper, the diameter and the overall length of the mill were measured to be 3.175 mm and 31.8 mm respectively. The figure on the right demonstrates the extruded cylinder.

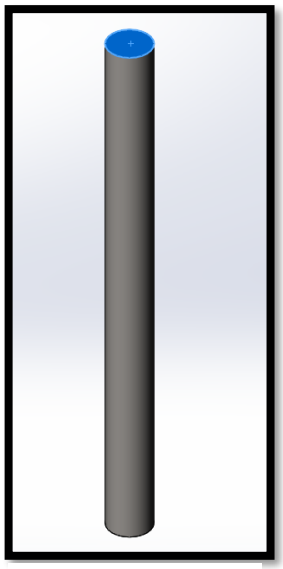

Figure 16 Extruded Cylinder

The top face of the cylinder (blue in figure 16) is flat, which worked out great for us since we are dealing with a flat end mill. The next task was to make

the flutes themselves. As seen in figure 17, the flutes have a rather complex helical shape. In order to fully understand how to produce these flutes on SolidWorks we decided to look at the manufacturing process of end mills, specifically the way the flutes are made. Our research led to the discovery that a computer-generated milling machine carves helix shaped ridges (the flutes) on to the end mill (figure 18). The number of these helical ridges and its length (the flute length) differ from end mill to end mill but they all follow the same process. So, using this information we realized that we can make the flutes using the swept cut feature on SolidWorks.

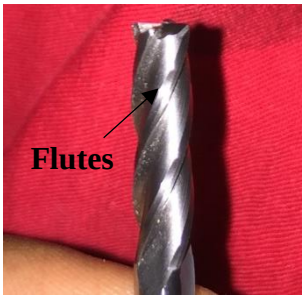

Figure 17 The flutes of our 1/8th inch End Mill

Figure 18 Manufacturing process of the flutes

In order to use the sweep-cut feature, we needed two things, a profile of the cut and its path. The profile is going to be the flute profile that we labeled back in figure 15. To get the flute profile, we tried scanning the end mill with its flat face facing down. However, since the end mill is very small, the resolution of the scan wasn't good and we couldn't get a good sense of the profile. A similar attempt was made on a photocopier but it also produced a low-resolution picture. So, we decided to take a picture of the top face of the end mill with a camera. Then we imported the picture on the top face of the cylinder and started scaling it down till the picture of the top face of the end mill matched with the diameter of the cylinder. After that was accomplished, we simply used splines and lines to trace out the profile. We only traced out one

of the profiles because we planned on using the circular pattern feature after the sweep cut is made. The figure on the right shows the flute profile sketch with the picture in the background, as it was overlaid in SolidWorks.

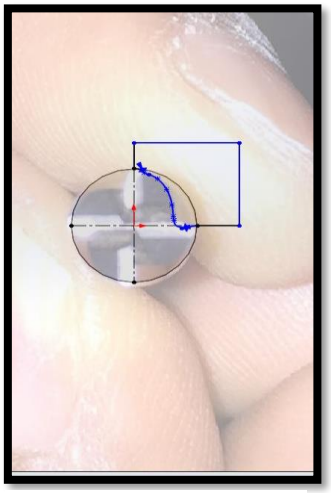

Figure 19: Flute Profile

Now that we have our profile, our next step would be to get the path. As discussed before, flutes follow this helical pathway along the end mill. Figure 20 shows what a helix looks like. So, to create that path, we first decided to draw a circle on the top face (blue in figure 2) that has the same diameter of the cylinder. After we had the circle we decided to use the helix and spirals feature on SolidWorks to create a helical path around the end mill, however we needed two pieces of information to use that feature. One of them was height and the other was number of revolutions. We noted that the flutes terminated after 0.75 turns so we used that as the value for number of revolutions. The height was just the flute length minus the smooth transition length (shown in figure 15) of the end mill which we measured using a caliper to be about 13.4 mm. Inputting these values into SolidWorks' helix feature, it gave us the helical shape shown in figure 21 below.

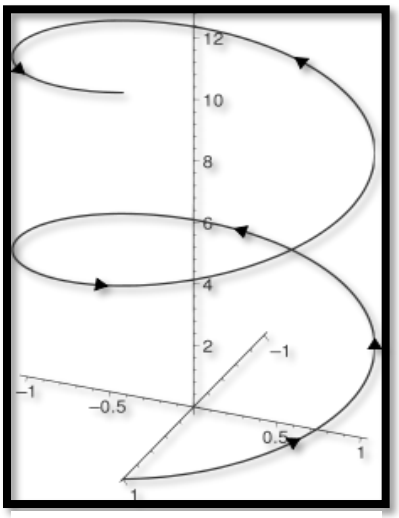

Figure 20 Helix

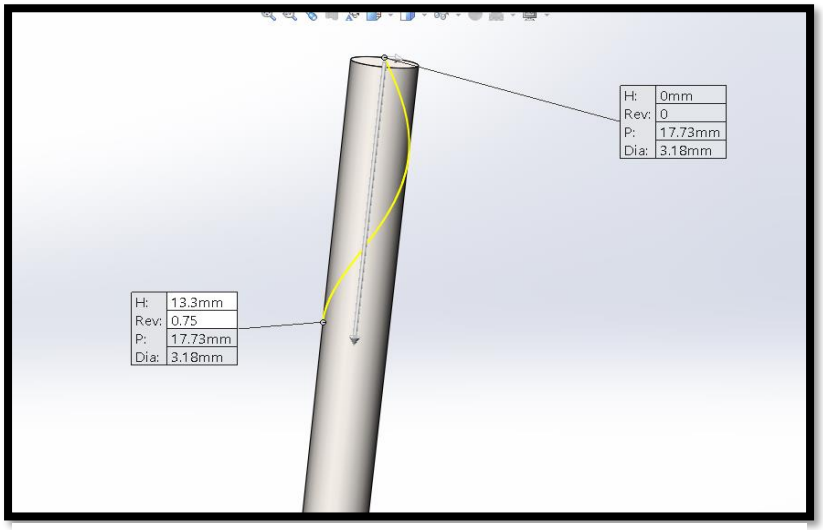

Figure 21 Helix Path creation

Now that we have the profile and the path, we can utilize the sweep cut feature to create the flute (figure 22). We needed three more flutes which we can make using the circular pattern feature, however before we can use that feature we had to create an axis that goes through the cylinder (figure 23).

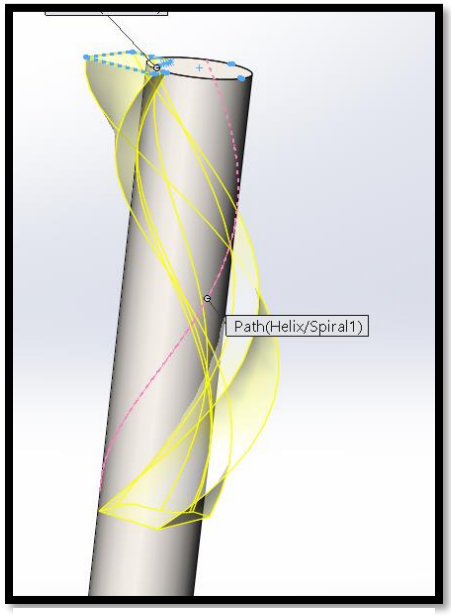

Figure 22 Cut Sweep

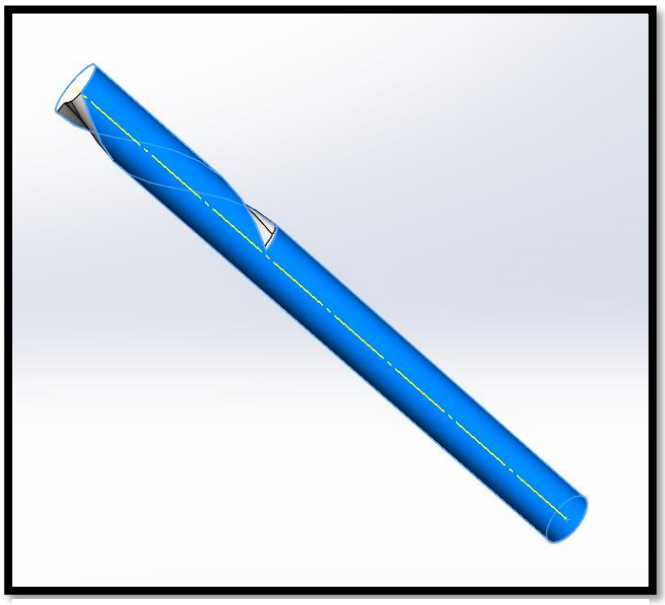

Figure 23 Axis Creation (Yellow)

Then using circular pattern of the sweep cut around that axis we created the model shown in figure 24 below.

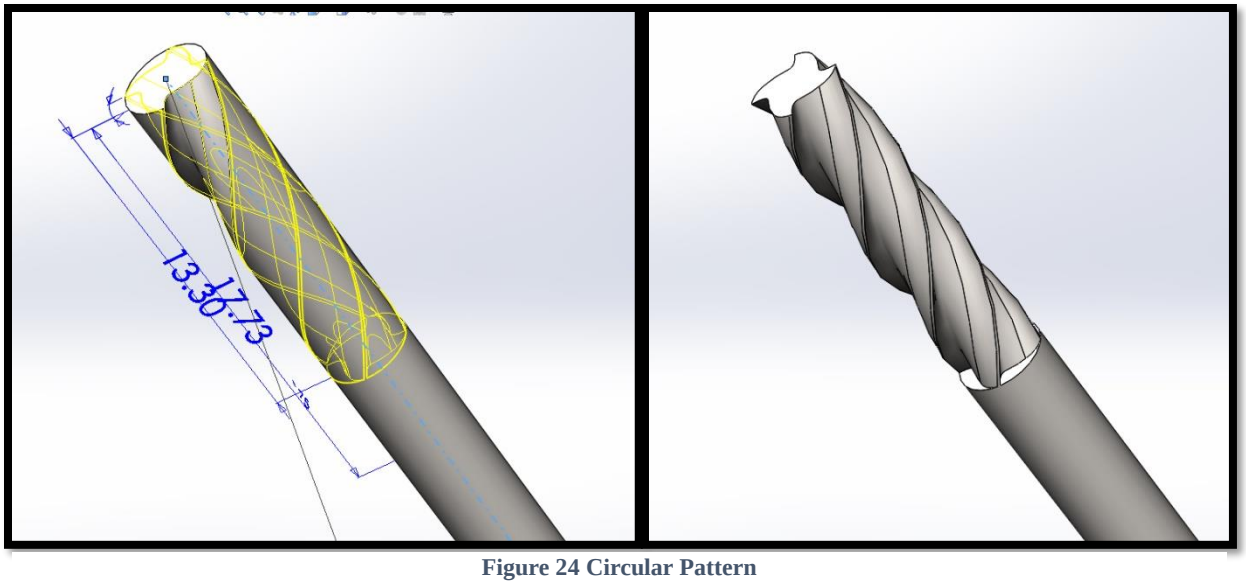

Figure 24 Circular Pattern

As seen on the figure on the right, there is a smooth transition from the flutes to the shank. However, our model so far doesn't really have that smooth transition (figure 25). So, we need to do another sweep cut to produce that smooth transition. We started off by selecting one of the faces where the flutes terminated (figure 26) and then used the convert entities feature to create a sketch on that face (figure 27). The sketch created will serve as the profile for the sweep cut feature.

Figure 25 Transition from the flutes to the shank

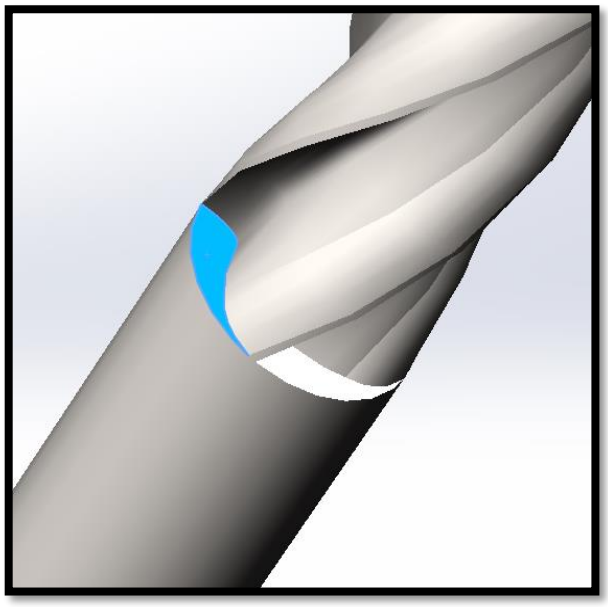

Figure 26 Selecting the face

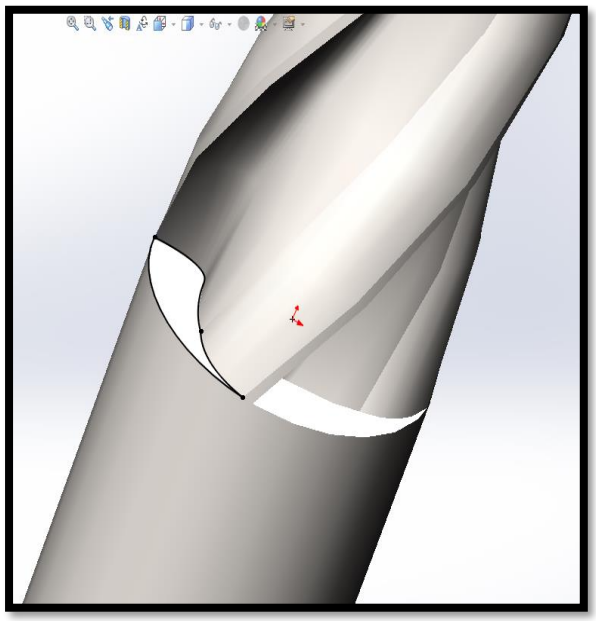

Figure 27 Convert Entities

Now to create the path, we followed the same steps as before and created a helix. However, unlike the previous helix, this helix is supposed to go outward, which we figured out by looking at the yellow profile shown in Figure 28. Using a protractor, we approximated the angle of that profile with the respect to the axis to be around 15°. Then using a caliper, we measured the length of the smooth transition and it came out to be around 1.1 mm shown in figure 28.

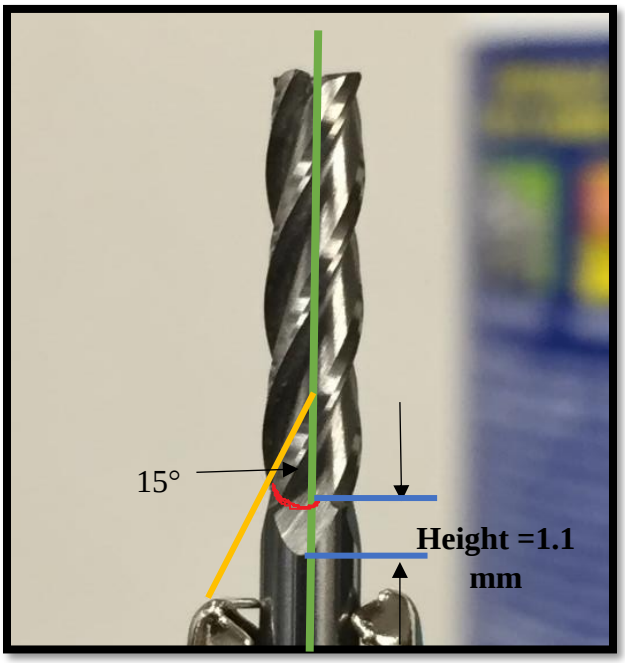

Figure 28 Measurements for the second sweep cut.

In order to create a helix that goes outward, we had to use the tappered helix feature and set it to 15° degrees that was measured earlier (Figure 28). Then we had to experiment with different revolutions and path lengths[1] to get a good approximation of the smooth transition. For each experiment, we measured the height of the smooth transition by measuring it using smart dimensions and then comparing it to the value from Figure 28. We repeated this process until we

[1] Path Length is different from the height measured in figure 14. The path length is the length of the helix which extends outwards. The "height" is the height of the smooth transition after the sweep cut has been done.

got a good approximated value for the height. We settled on 0.25 revolutions with a path length of 10 mm (Figure 29).

We also decided to use the “follow path” option in the cut sweep feature so that the cut follows the same path as the previous sweep. Then using the circular pattern feature about the axis drawn before (figure 23), we get the sweep cut for the smooth transition shown in figure 30.

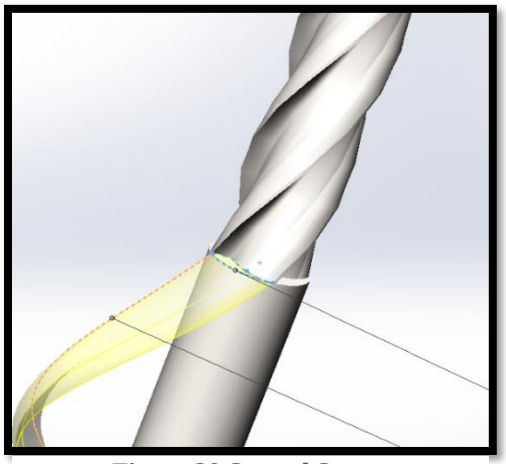

Figure 29 Second Sweep

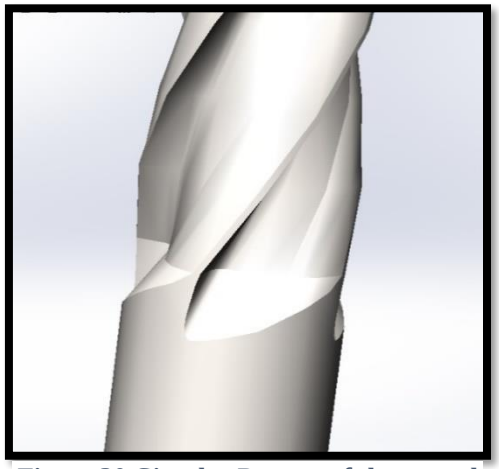

Figure 30 Circular Pattern of the second

A picture of the real end mill is shown on the right and the rendered solid model is shown on the left for comparison.

Figure 31 Solid Model (Left) vs The real End Mill (Right)

Defeaturing

As mentioned before in the problem statement, we will be modeling the end mill as a cantilever beam deflection. We don't necessarily need to include the details shown in figure 32 because, the load paths connect the applied forces to reaction forces and do not concentrate through the web or face of the end mill. Not only it will simplify the overall model and eliminate any unnecessary stress concentrations but also save run time. So, we decided to stick with the flat face shown in figure 33.

Figure 32 Detailed top face

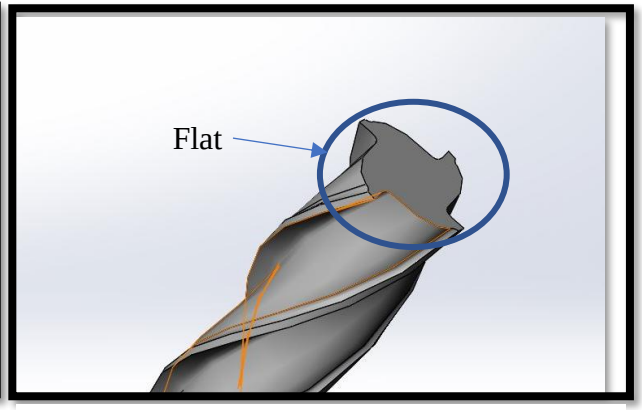

Figure 33 Defeatured top face

Analytical Results

To have a better understanding of what was happening to the end mill when it was being used, we compared the end mill to a cantilever beam. There was a force applied to the end mill labeled P and shown is figure 34. The deflection is approximately to be 0.59mm and labeled as δ_{max}. The total length of the end mill is 21mm, which in this case is the defeatured length of end mill used here, or better known as the length of then end mill outside of the collet, further explained in boundary condition section. By applying the formula developed in an ASME paper published in 2003 titled Development of an Analytical Endmill Deflection and Dynamics

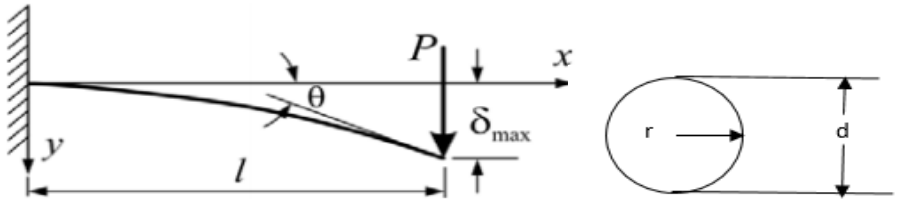

Figure 34: Diagram of a Cantilever Beam

Model[2], we solved for an approximation of the force P, acting on the end mill. Figure 34 shows a cantilever beam which the endmill is model is developed from, and figure 35 shows the boundary conditions and loadings of the endmill.

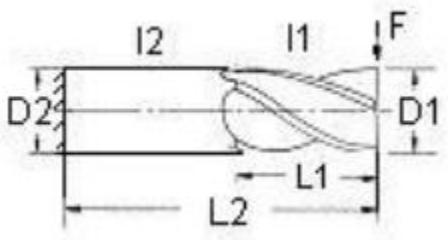

Figure 35 Boundary Conditions and Loading of the Endmill in our analytical model

In figure 35, D1 is the diameter of the flute and *D2* is the diameter of the shaft. F is the force applied to the end of the end mill which is a point load. For later reference, the force will be denoted as P. L1 and L2 are the length of the flute and total length of the endmill respectively. Finally, I1 and I2 are the second moment of area of the cross sections of the flute and shaft respectively. For a cantilever beam, only one second moment of area is used to calculated deflection, but for this instance, we need to factor in the flute of the endmill which has its own second moment of area. By including two different second moments of area, for the shaft and flute, we will obtain an approximate force acting on the end mill. For our case, we know the maximum deflection but we don't know the force applied on the end mill. From the formula provided in the research paper published by ASME in 2003, we can solve for the force. The data and formulas below show how we obtained the force denoted as P.

We have several known values for the boundary conditions of the endmill. What we know is the length of the flute, the total length of the endmill, the total deflection of the endmill, the diameter and radius of the endmill and the modulus of elasticity of the material of the endmill which is Tungsten Carbide.

[2] Development of Analytical Endmill Deflection and Dynamics Models, ASME 2003

$$Length\ of\ flute: l_1 = 13.3\ mm$$

$$Total\ length\ of\ the\ endmill:\ l_2 = 21\ mm$$

$$Maximum\ Deflection: \delta_{max} = 0.59\ mm$$

$$Diameter: d = 3.175\ mm$$

$$Radius: r = 1.5875\ mm$$

$$Modulus\ of\ Elasticity: E = 675{,}000\frac{N}{mm^2} = 675\ GPa$$

What we don't know is the force that is applied on the end mill. But knowing the formula for deflection we can solve for the force P. Before we do that, we need to solve for other variables in which we can use to obtain the force from the deflection formula. I_1 is the second moment of area of the flutes which was obtained through SolidWorks section properties evaluation, figure 36.

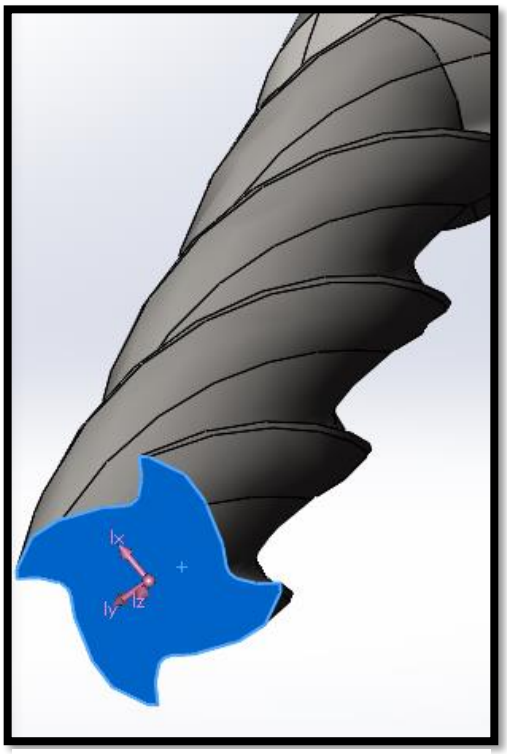

Figure 36 Highlighted blue face is the evaluated section for second moment of area

I_2 is the second moment of area of the shaft. Their formulas are shown below.

$$I_2 = \frac{\pi r^4}{4} = \frac{\pi(1.5875mm)^4}{4} = 5mm^4$$

The deflection formula for a simple cantilever beam is $\frac{Pl_1^3}{3EI_1}$, but for the case of an endmill, we need two more factors that are added to the original deflection. Those two factors that are added to the deflection formula, include considerations for the deflection due to the flute and the shaft. The formula is shown below:

$$\delta_{max} = \frac{Pl_1^3}{3EI_1} + \frac{1}{6}\frac{Pl_1(l_2 - l_1)(l_2 + 2l_1)}{EI_2} + \frac{1}{6}\frac{Pl_2(l_2 - l_1)(2l_2 + l_1)}{EI_2}$$

When we solve for P we get the following formula.

$$P = \frac{\delta_{max}}{\left[\frac{l_1^3}{3EI_1} + \frac{l_1(l_2 - l_1)(l_2 + 2l_1)}{6EI_2} + \frac{l_2(l_2 - l_1)(2l_2 + l_1)}{6EI_2}\right]}$$

Now we are able to plug in the known values of the variables used in the formula for P. This is shown below. The value for P obtained is 486N.

$$P = \frac{0.59mm}{\left[\frac{(13.3mm)^3}{3\left(\frac{675{,}000N}{mm^2}\right)(2.18mm^4)} + \frac{13.3mm(21mm - 13.3mm)(21mm + 2 * 13.3mm)}{6\left(\frac{675{,}000N}{mm^2}\right)(5mm^4)} + \frac{21mm(21mm - 13.3mm)(2 * 21mm - 13.3mm)}{6\left(\frac{675{,}000N}{mm^2}\right)(5mm^4)}\right]}$$

$$P = 486N$$

We now have an analytical approximation of the force acting on the endmill.

Boundary Condition

To begin static studies on the end mill, we need to determine the boundary conditions and where to place the boundary condition. To determine the boundary conditions, the first thing we do is analyze the end mill inside of the collet. A certain length of the shaft of the end mill is

Figure 37 Collet

placed inside the collet and a certain length of the shaft is outside of the collet. The length of the shaft fixed inside of the collet will be used as a fixed restraint. Figure 37, on the previous page, depicts a collet with a broken 3/16th inch end mill in it. The length of the end mill inside of the collet stayed fixed while the rest of the end mill broke off.

From the figure on the previous page, we can determine where our first boundary condition will be placed. To determine the length of the fixed portion, we used our observation of the 1/8th inch end mill in the collet and applied it to the solid model of the end mill. This can be seen in Figure 38 below. In the solid model, we used the split line feature to project a line on the surface of the end mill to show the length of the shaft inside of the collet. The blue shaded area is the length of the shaft inside of the collet which is 17.15mm. We used a fixed restraint, seen in Figure 38, on the blue shaded area to illustrate the restraint on the end mill.

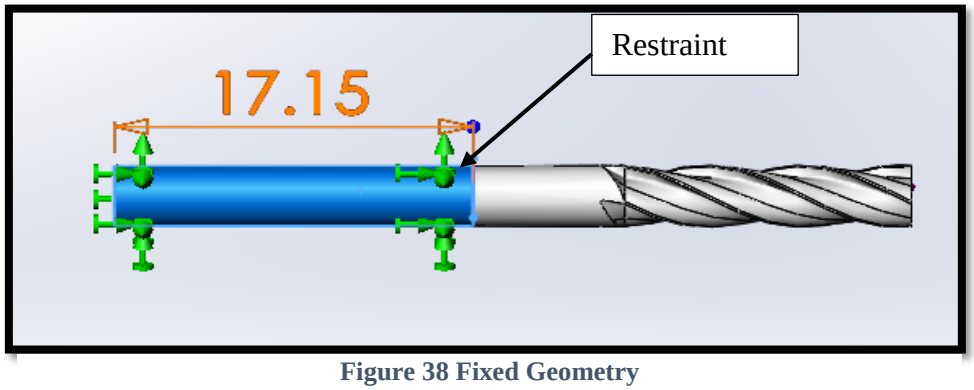

Figure 38 Fixed Geometry

Boundary Condition Forces

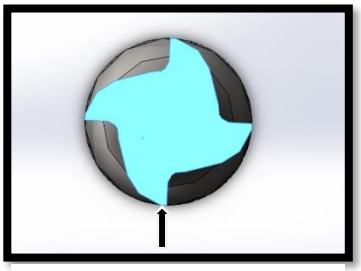

Figure 39 Forces on an endmill

Now that we know where to apply the force, we needed to know at what depth of the end mill we should apply the force. Since the end mill was cutting the stock at a depth of 0.03 inches (30 mils), we had to apply the force along that depth of the end mill. From figure 40 we can see where the force is applied. We used the split line feature to project a line at this area on the end mill which is shown in figure 41.

The cutting face of the flute of the end mill, comes into contact with the stock. Knowing that the depth is 0.03 inches, we can apply a force at this specific location as described in figure

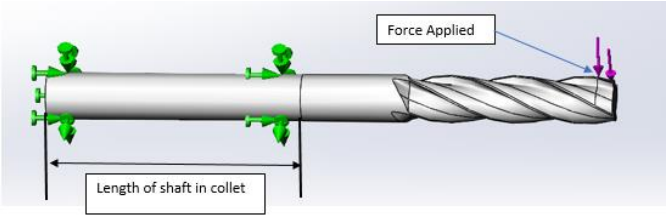

Figure 40 Application of force

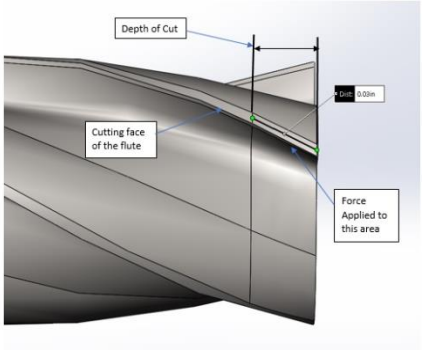

Figure 41 Split Line

40 which is the depth of cut. What we don't know is the force that is acting on the end mill at this location. Since SolidWorks is a linear solver, we can correlate the results of displacements for what magnitude of force would have caused the observe 590-micron displacement. Therefor a quasi-arbitrary value was chosen for the force applied at the area specified in Figure 31 is 500 Newtons. The value of 500 is arbitrary but close to the analytical result of the force, 486 N, making it quasi-arbitrary. Figure 42 and 43 shows a closer look to where we applied the 500 Newton force.

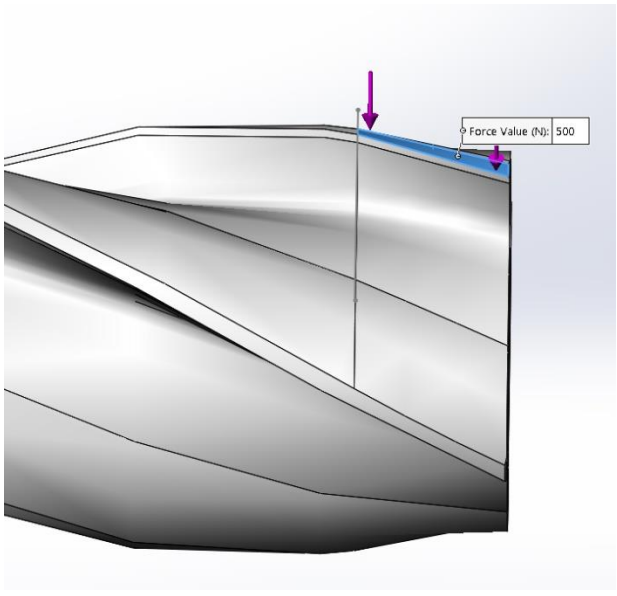

Figure 42

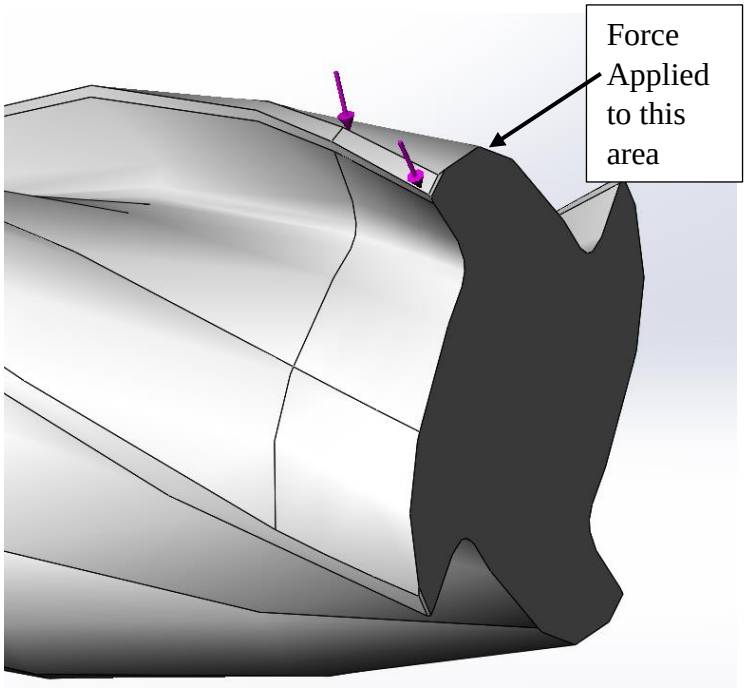

Figure 43

Boundary Condition (Continued)

To save nodes and elements as well as decrease run time, we decided to further defeature the solid model. Instead of applying a fixed restraint on the shaft of the end mill, we decrease the shaft length of the end mill and applied a fixed restraint on the flat face of the end mill. The location we applied the fixed restraint to the flat face, simulates the area of where the end mill sticks out of the collet. We can see where the fixed restraint is placed in figure 33 and we can also see the new length of the end mill.

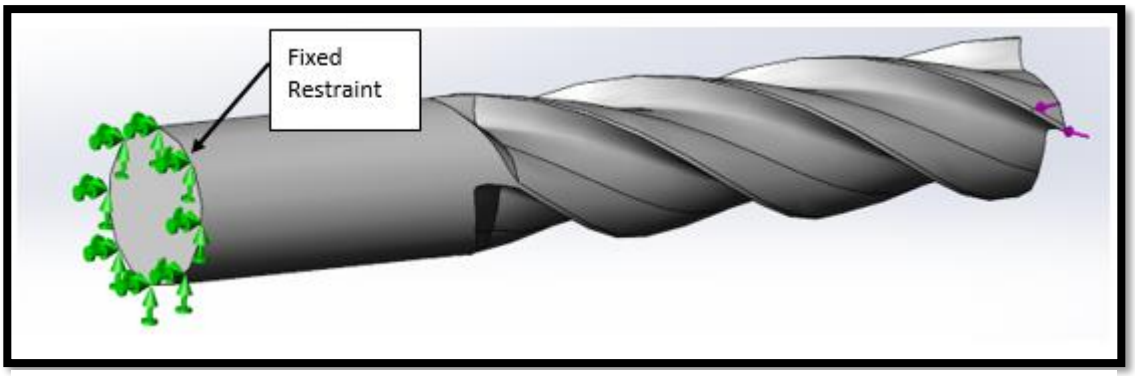

Figure 44 New Fixed Restraint

Meshing

Standard second order tetrahedral elements were used with global h-refinement. The reason for only global refinement is that there were many areas of interest throughout the endmill which would have required local refinement. The fluted section of the endmill has substantial changes in geometry which could cause stress concentrations to arise and this section is more than half the axial length of the FEA endmill model. Since the stress at the fixed geometry, representing the collet fixture, was also of interest, the elements in that region would have to be included for refinement as well, otherwise the stress calculated would be a false-convergent value. The element sizes chosen ranged from 0.7mm to 0.3mm, as shown in Figure 45. The same refinement technique was used for each subsequent study.

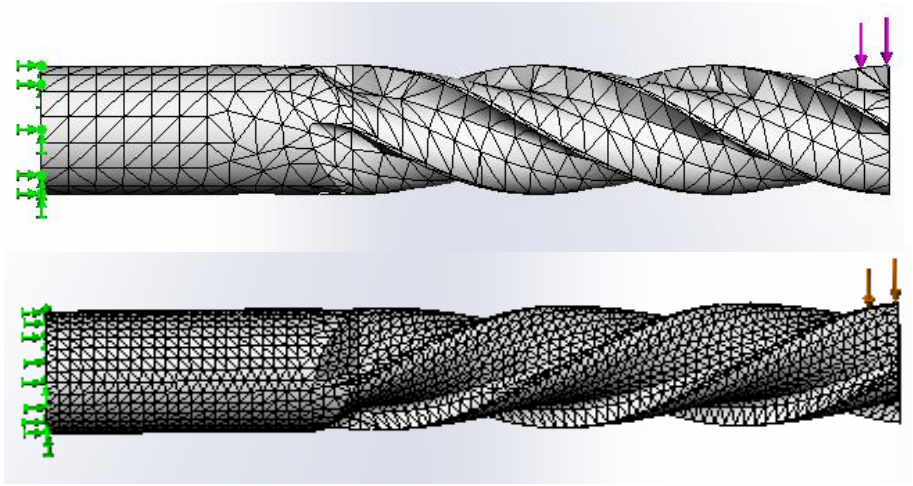

Figure 45 Second order standard tetrahedral elements used in all studies. The largest element size of 0.7mm shown on top and the smallest of 0.3mm shown on bottom.

Singularity

After applying the mesh and running the simulation, we noticed two stress hot spots. One of those stress hot spots was located at the collet and the other was located around the area of smooth transition from the flutes to the shank (Figure 46). The locations of these stress hot spots lined up quite nicely with the predictions that we made beforehand. Using the probe results feature, we probed the nodes in those stress hot spots in order to get a good sense of the values of maximum stress. Then we did a convergence tests for both of those stress hot spots. The maximum stress around the smooth transition area converged nicely to an approximated finite value with mesh refinement, however the maximum stress near the collet kept on increasing with mesh refinement. This section will focus on why that might be happening and what is the best way to resolve the issue. A diverging maximum stress value with h refinement are not indicative of stress concentrations. In fact, they are the characteristic behavior of stress singularities. Those maximum stress values are theoretically diverging to infinity with mesh refinement. And in real life there is no such thing as infinite stress. In FEA divergence and singularities are a common factor, but that doesn't necessarily mean we disregard them or ignore them. Singular stresses are not real but their existence can tell us a lot about the FEA model itself, so it is always a great idea to analyze and learn from divergence data. Below is a zoomed in figure of the stress singularity at the collet.

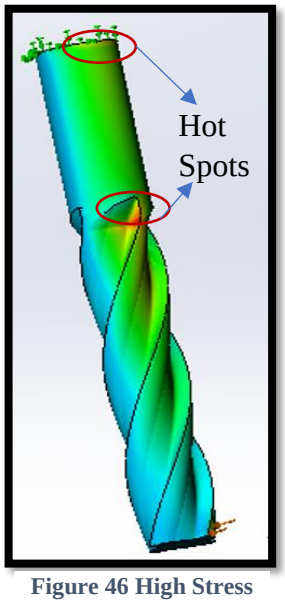

Figure 46 High Stress locations

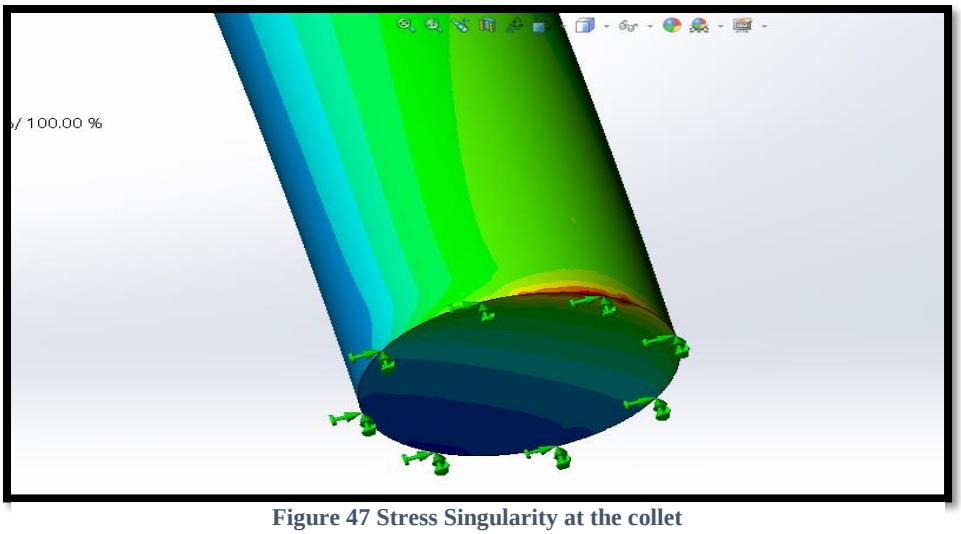

Figure 47 Stress Singularity at the collet

A singularity usually occurs when there are sudden discontinuities in geometry or when there are sharp edges. But we weren't sure if that was the case for our end mill, so we first decided to look into what is exactly happening at the singularity area by looking at the elements in that area.

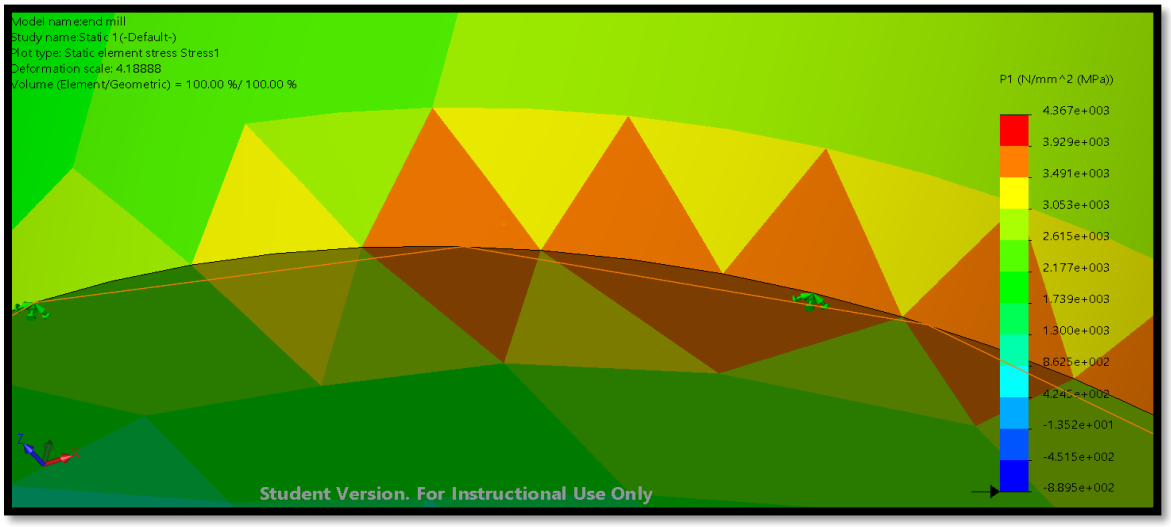

Figure 48 Looking at the stress elements near singularity.

Using the advanced option in the stress plot menu, we selected to show element values. Then we zoomed into the area of singularity (Figure 48). This analysis was done with a 0.3 mm global standard mesh. As seen from the figure above, the stresses are not distributed properly and too much of a jump between element stress values (indicative by the different colors) is never a good sign. The FEA model is based off an incorrect mathematical representation. The stresses in adjacent elements should not be so drastically different. So, now the question arises why is this singularity happening.

The singularity occurred because the restraint suddenly ended. The real endmill is continuous through the fixture, only the FEA model is discontinuous so only the FEA model has a stress singularity. As mentioned before singularities are a common thing in FEA and sometimes we have to know when to ignore them. Usually they can be ignored if we are interested in an area that is far away from the singularity, however for our case we are actually interested at the stresses at the singularity. So, we decided to use values of stresses a little bit away from the singularity by using the probe feature.

Nodal Probing

In order to obtain a convergent stress value for the collet region, we employed a technique of nodal probing, using the Probe feature, as seen in Figure 49. The nodal stress values along the fixed restraint are much greater than the nodes on the same elements not coincident with the restraint. The nodal values of stress within the same element are vastly different, which is what previously indicated to us a stress singularity. The tier of nodes closest to the fixed restraint (collet), but not coincident with it, were probed for stress values. The node with maximum stress was taken as the value of stress "at the collet". Figure 49 shows three probed nodes not coincident on collet and how the chosen maximum stress value (circled in red) is obtained by having two lower values of nodal stress adjacent on either side.

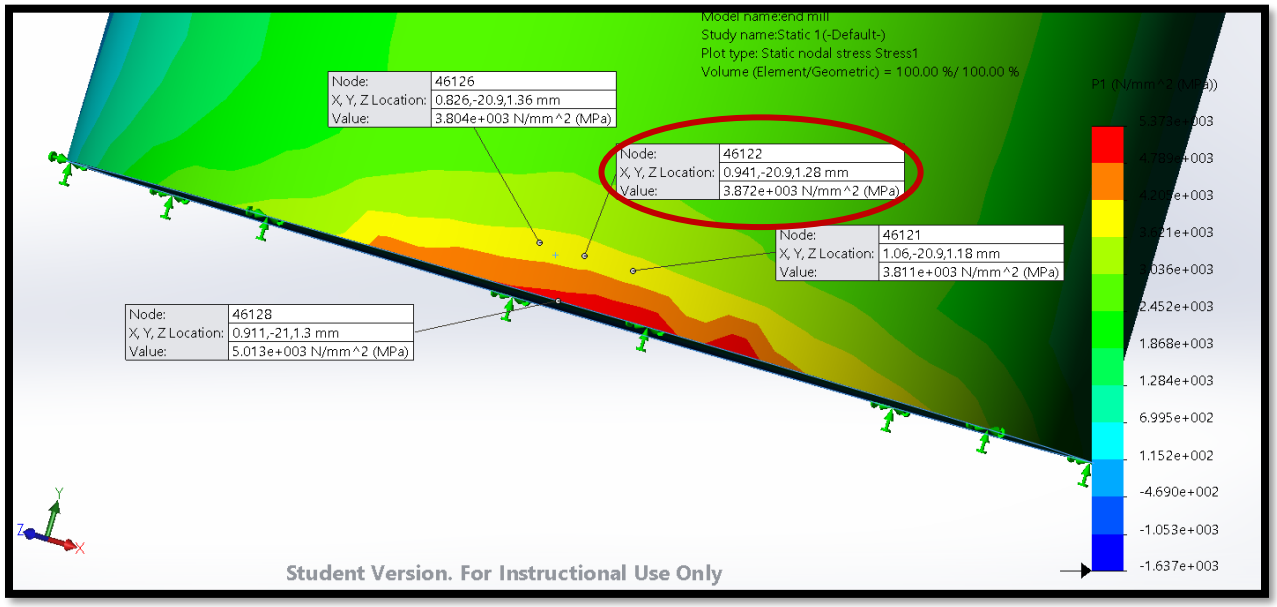

Figure 49 Nodal Probing

SolidWorks as Linear Solver

By the nature of SolidWorks as a linear solver we do not need to perform more studies to see what value of force will produce the displacement which was observed. For whatever arbitrary force, we apply we can linearly appropriate the deflection that would be caused by the arbitrary force to find the force which would have cause the observed displacement. Once the factor of appropriation is calculated all inputs and outputs of the simulation studies can be manipulated by this factor to give values of stress that representatively approximate the endmill which we observed fracturing. In order to properly provide a recommendation for the depth of cut, several studies with varied depths of cut will be run to obtain a relationship between the depth of cut and the first principal stress developed. When the stock is forced upon the cutting edge of the endmill, the force the stock exerts on the endmill is distributed over the area of contact. The load is assumed to be distributed evenly, so that the cutting depth and the incident force are proportional, so that if the cutting depth is halved, the applied force would be halved as well. The simulated cutting depths are 30, 15, and 2 mils, with respective arbitrary applied forces of 500, 250, and 33.3 N. A schematic of the different loading conditions is shown below in Figure 50.

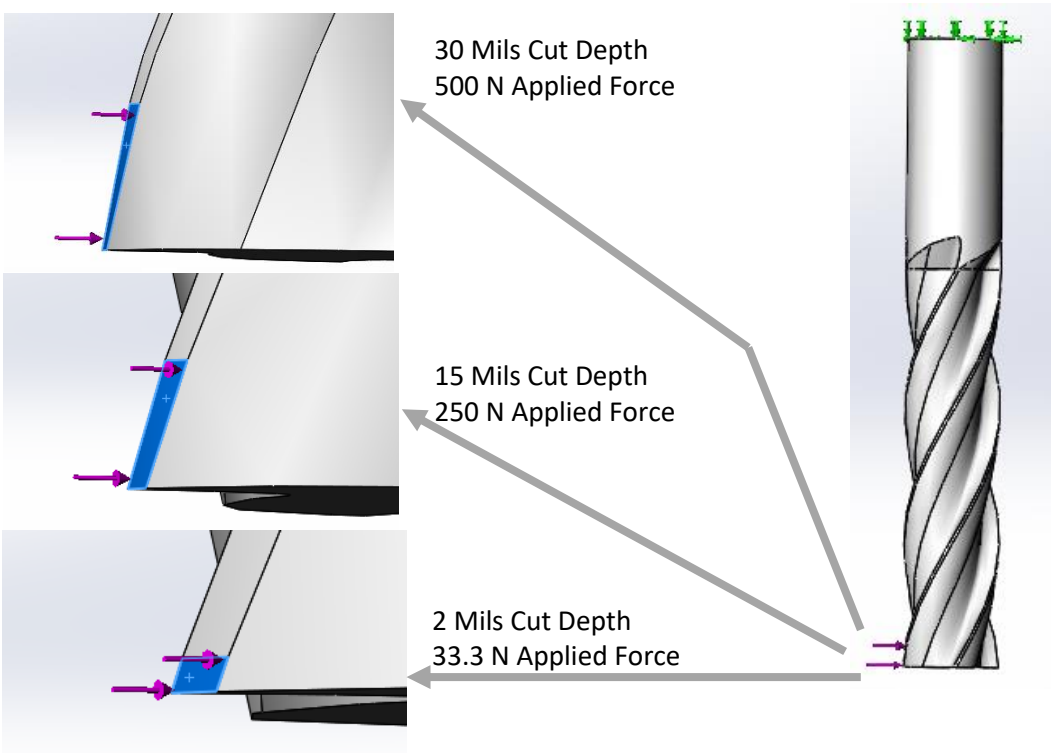

Figure 50 Different Loading Conditions

Results

The results and parameters of all three studies are shown and tabulated in Table 1. For each study, the 1st principal stress plot is shown for the coarsest mesh (0.7mm global element size) and the finest mesh (0.3mm global element size), as well as convergence plots. The results obtained for stress and displacement are for arbitrary force inputs and are not directly representative of the endmill and conditions it was actually used in. The force inputs, and stress/displacement outputs will be linearly appropriated so that the (appropriated) displacement from the simulation would be representative of the observed deflection.

Table 1 Results

	#	#	#	mm	(GPa)		microns	seconds
	# of Elements	# of Nodes	DOF	Global Element Size	Stress Concentration	Stress at Collet	Max Displacement	solve time
500N	3337	5732	16962	0.7	4.94	3.2	647	4
30 Mils Cut	5686	9511	28164	0.6	5.31	3.46	668	6
	8023	13074	38766	0.5	5.25	3.23	672	8
	15504	24051	71475	0.4	5.51	3.71	679	15
	21095	32469	96450	0.35	5.47	3.78	680	18
	33859	50923	151566	0.3	5.69	3.61	680	30
250N	3303	5691	16839	0.7	2.61	1.63	330	2
15 Mils Cut	5639	9444	27963	0.6	2.74	1.75	341	3
	7848	12831	38037	0.5	2.71	1.64	343	4
	15555	24127	71703	0.4	2.86	1.863	347	8
	20912	32231	95736	0.35	2.88	1.9	348	9
	33770	50788	151161	0.3	2.94	1.85	348	14
					(MPa)	(MPa)		
33.3 N	3333	5730	16956	0.7	350	219	40	2
2 Mils Cut	5668	9480	28071	0.6	371	234	47	3
	7833	12843	38073	0.5	373	217	47	3
	15611	24230	72012	0.4	393	253	48	6
	20904	32243	95772	0.35	391	257	48	8
	33957	51067	151998	0.3	403	250	48	13

30 Mils Cut Depth – 500 N Applied Force

Convergent Value for 1st Principal Stress at Collet – 3.75 GPa

Convergent Value for 1st Principal Stress at Concentration – 5.60 GPa

Convergent Value for Resultant Displacement – 680 Microns

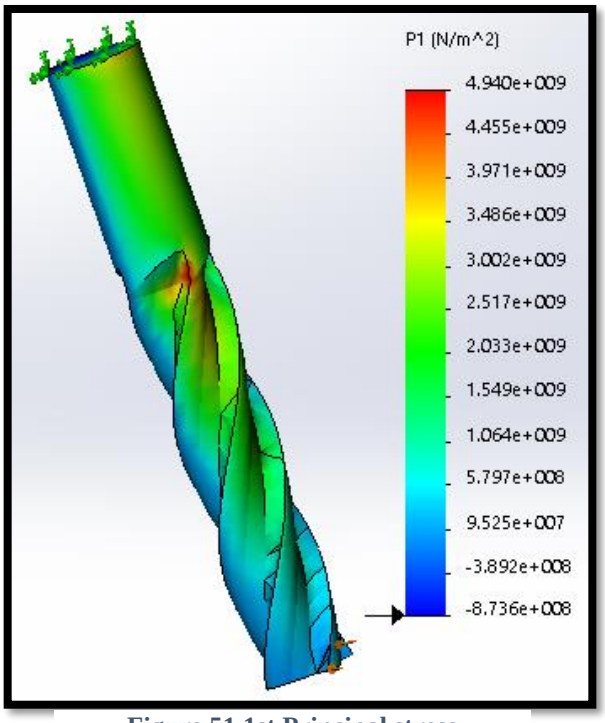

Figure 51 1st Principal stress distribution. 30 Mils cut depth, 500N applied force. 0.7mm global element size.

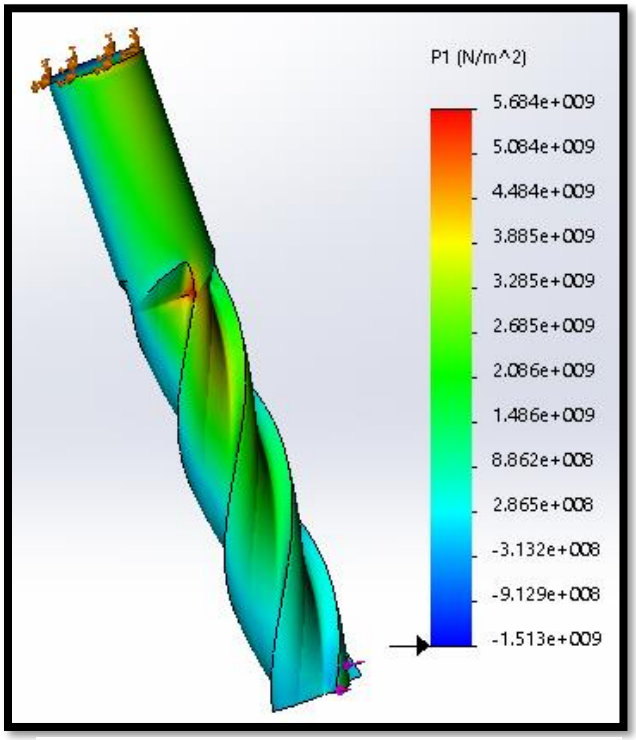

Figure 52 1st Principal stress distribution. 30 Mils cut depth, 500N applied force. 0.3mm global element size.

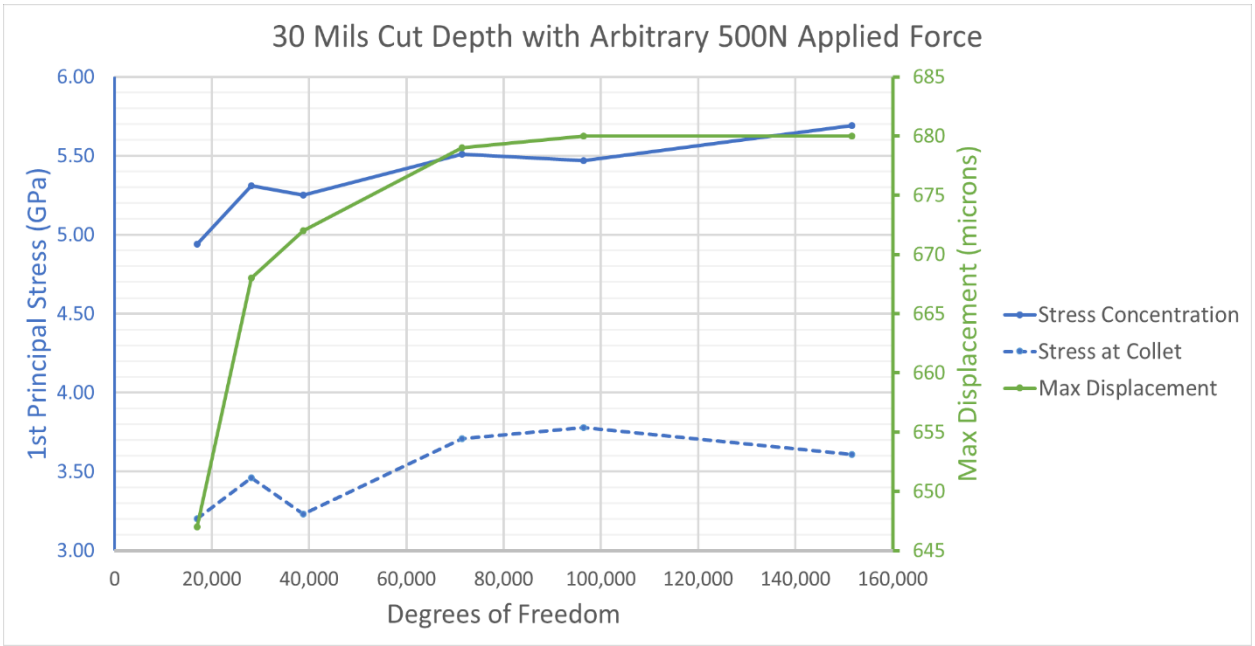

Figure 53 30 mils cut depth with 500N applied force. Convergence plots for 1st principal stress and displacement vs degrees of freedom

15 Mils Cut Depth – 250 N Applied Force

Convergent Value for 1st Principal Stress at Collet – 1.90 GPa

Convergent Value for 1st Principal Stress at Concentration – 2.80 GPa

Convergent Value for Resultant Displacement – 348 Microns

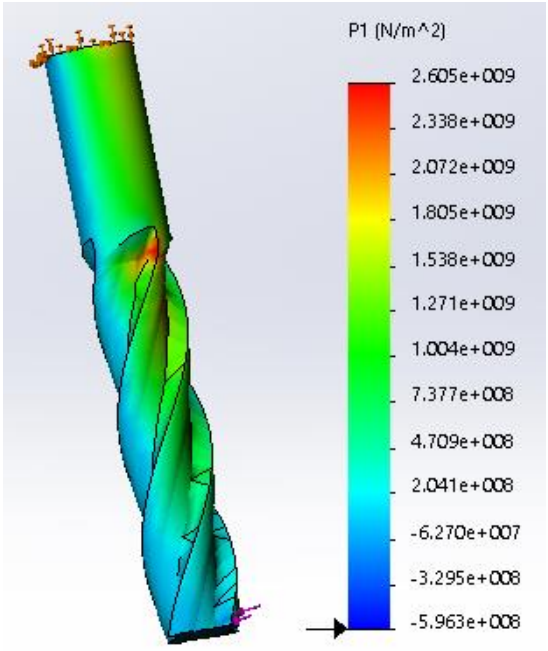

Figure 54 1st Principal stress distribution. 15 Mils cut depth, 250N applied force. 0.7mm global element size.

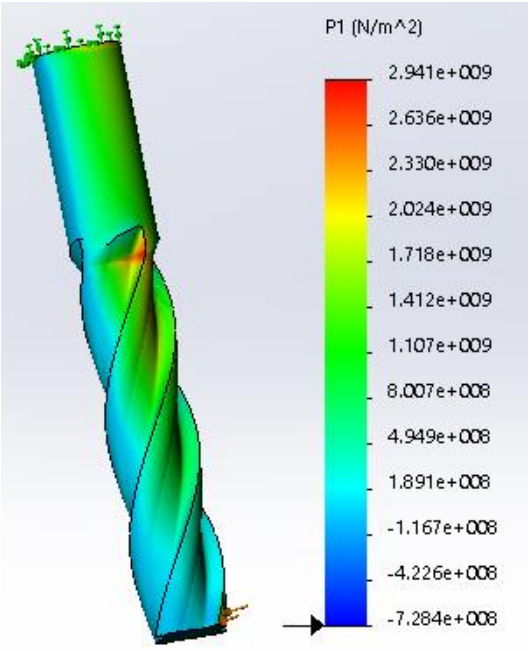

Figure 55 1st Principal stress distribution. 15 Mils cut depth, 250N applied force. 0.3mm global

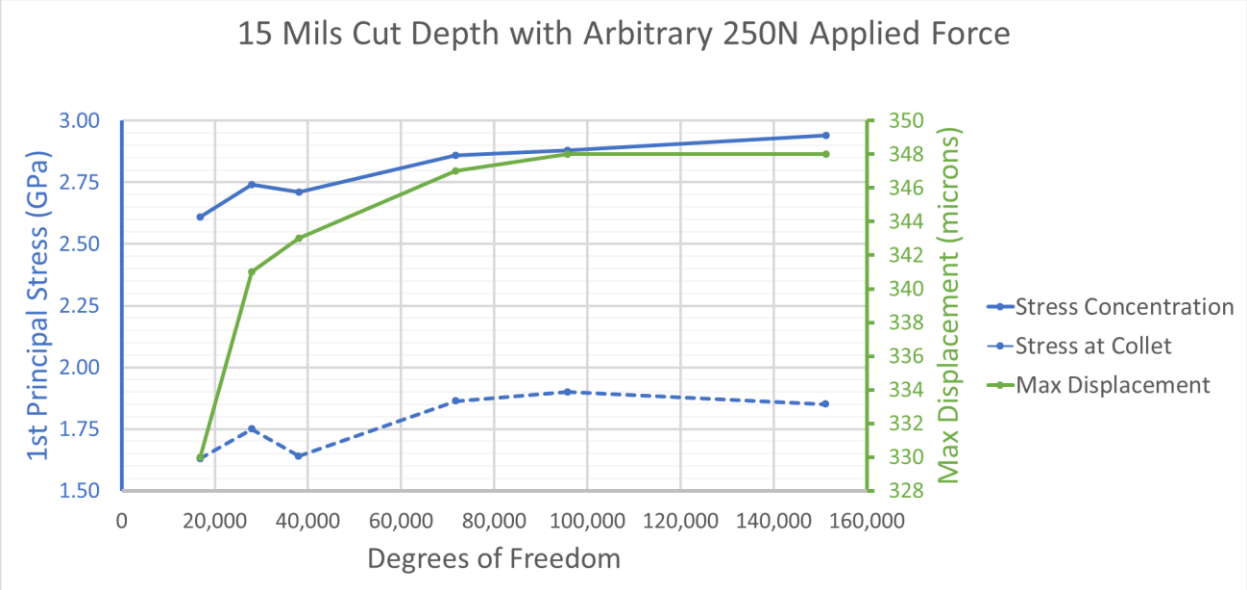

Figure 56 15 mils cut depth with 250N applied force. Convergence plots for 1st principal stress and displacement vs degrees of freedom.

2 Mils Cut Depth – 33.3 N Applied Force

Convergent Value for 1st Principal Stress at Collet – 250 MPa

Convergent Value for 1st Principal Stress at Concentration – 390 MPa

Convergent Value for Resultant Displacement – 48 Microns

The stress distribution for the smallest cut depth of 2 mils showed to be different than the previous studies, as the color shows in Figures 59 and 60(next page). Upon closer inspection, it appeared as though a stress singularity had developed near the application of the force loading. The most probable cause of the singularity is that the force loading is being applied to a very small area, approximately 6,000 square microns. Due to the small area, the elements in that region are small in number and large in aspect ratio, as seen in Figures 57 and 58, therefore the stress at the area of force application is neglected and assumed to be an artificial stress. The stress values for the region of the concentration where the flute meets the shaft were obtained by probing the entities near it for the maximum stress value. The stress at the collet was obtained using the same previously mentioned nodal probing technique.

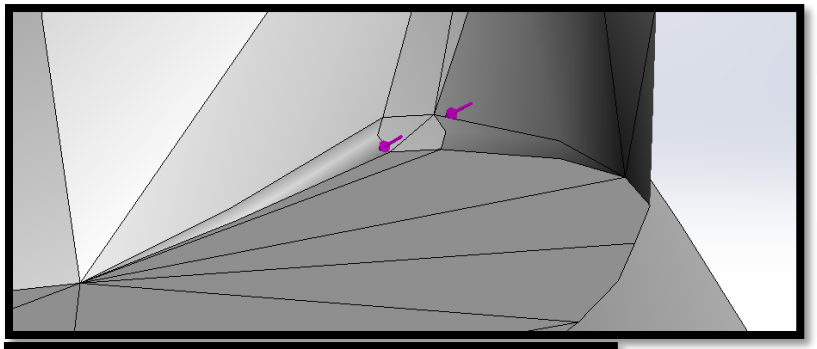

Figure 57 0.7mm Global Mesh, 2 Mils cut. Close up of mesh elements in small area where force (purple arrows) is applied.

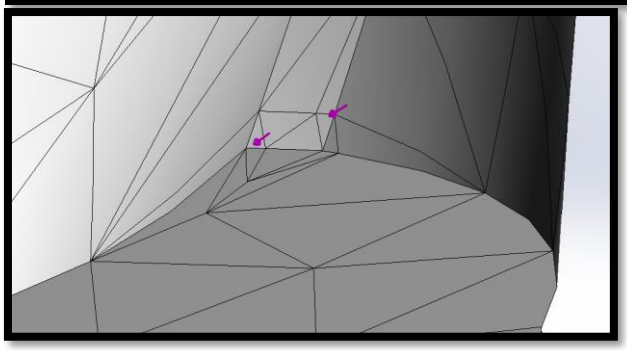

Figure 58 0.3mm Global Mesh, 2 Mils cut. Close up of mesh elements in small area where force (purple arrows) is applied.

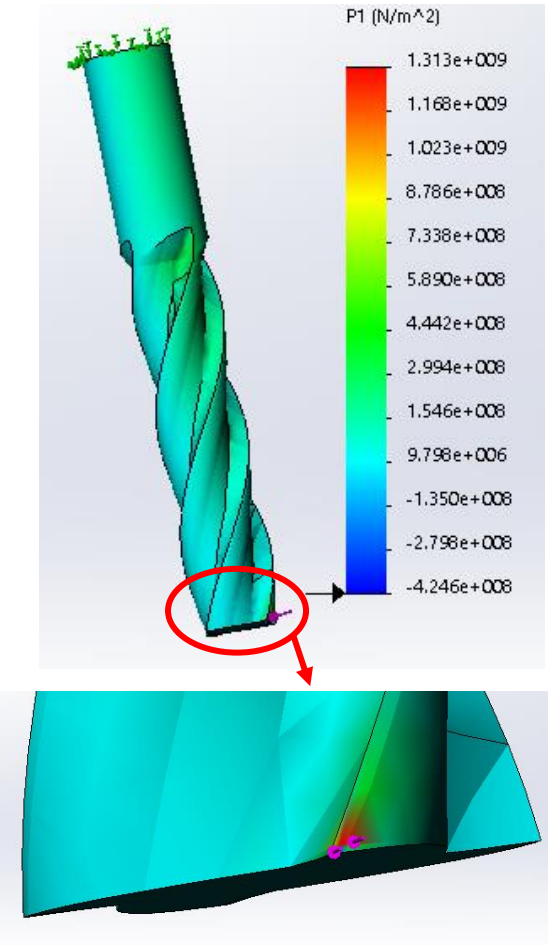

Figure 59 1st Principal stress distribution. 2 Mils cut depth, 33.3N applied force. 0.7mm global element size.

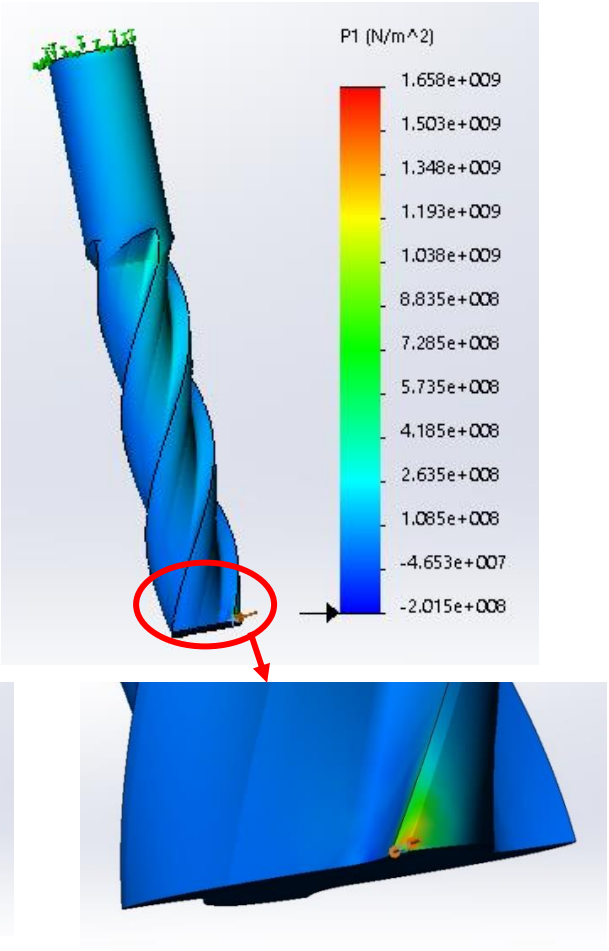

Figure 60 1st Principal stress distribution. 2 Mils cut depth, 33.3N applied force. 0.3mm global element size.

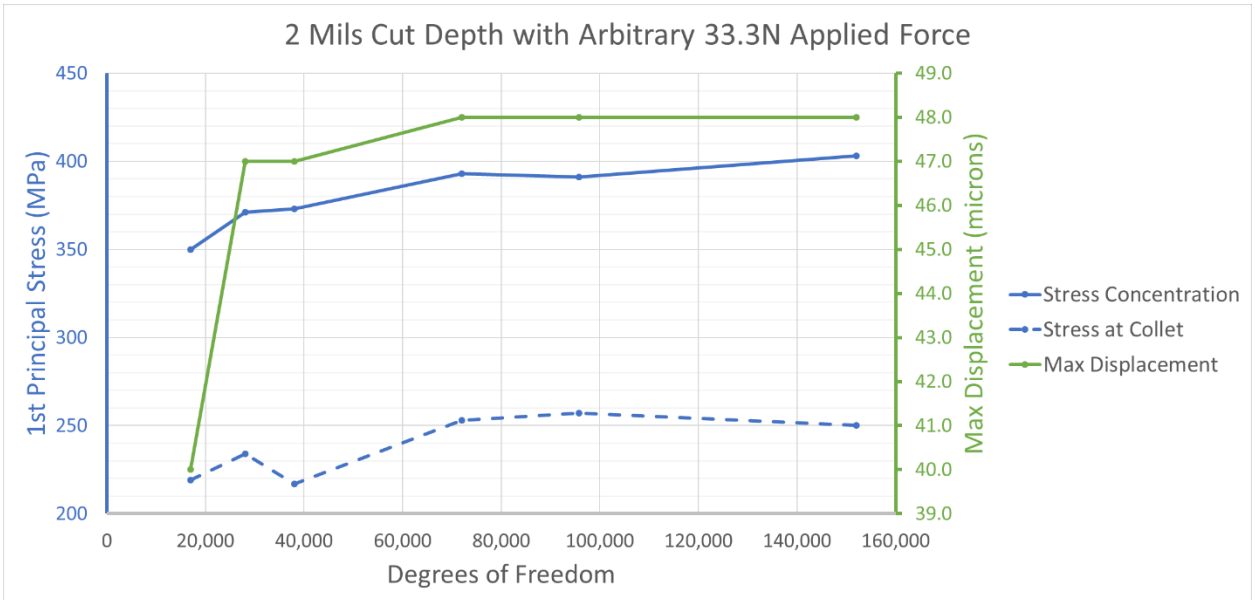

Figure 61 2 mils cut depth with 33.3N applied force. Convergence plots for 1st principal stress and displacement vs degrees of freedom.

Comparison of Cutting Depths with Arbitrary Forces

After convergent values of stress had been obtained for the region of the concentration and the collet, using the arbitrary applied forces, the values were plotted so that a relationship could be observed. The plot is shown in Figure 62, and it is seen that the values of stress behave linearly with the change in cutting depth; however, the linear behavior is different between the collet and the concentration. This shows that the distribution of stress changes as the cutting depth does, at larger cutting depths the stress is much greater at the concentration than at the collet, whereas the stress is more evenly distributed between the collet and the concentration at lower cutting depths.

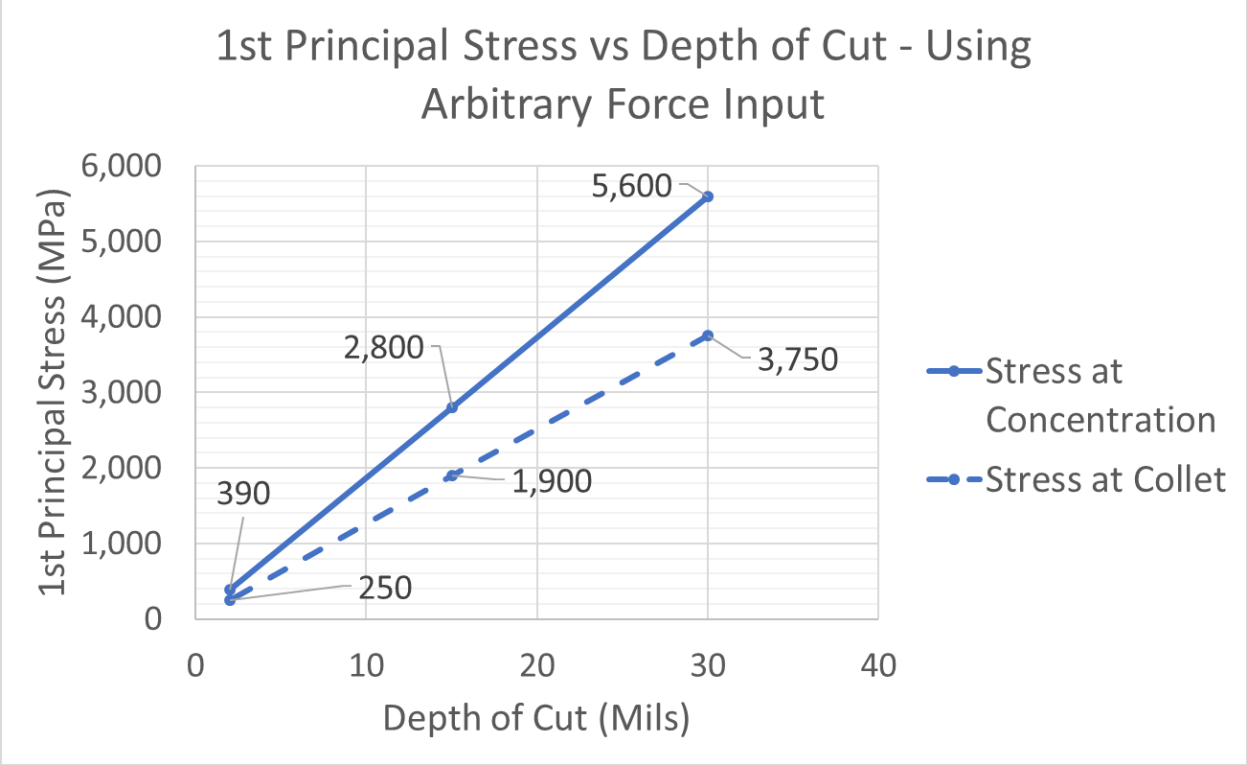

Figure 62 Different linear behavior of the stress that develops at the collet and at the stress concentration

Linear Appropriation

The displacement from the first study, 30 Mils cut depth and 500 N applied force, was used to find the factor of linear appropriation. A picture of a vector plot of the resultant displacement, zoomed in on the maximum displaced region, is shown in Figure 63. The maximum displacement from this simulation study was 680 microns, where the observed displacement from the endmill which was video recorded was 590 microns. The observed displacement, 590 microns, is about 87% of the simulated displacement, 680 microns; therefore, the force which would have caused the observed displacement of 590 microns would be 87% of the 500N arbitrary applied force in the simulation, or 435 N. This is taken to be validated by having only about a 10% error with the analytical solution of 486 N. The first principal stresses obtained from the simulations for all three studies is now appropriated by 87% to give a approximation of the stress developed in the endmill we observed to fracture. The values are tabulated in table below. The following page shows the graph of the appropriated stress with respect to the depth of cut, Figure 64.

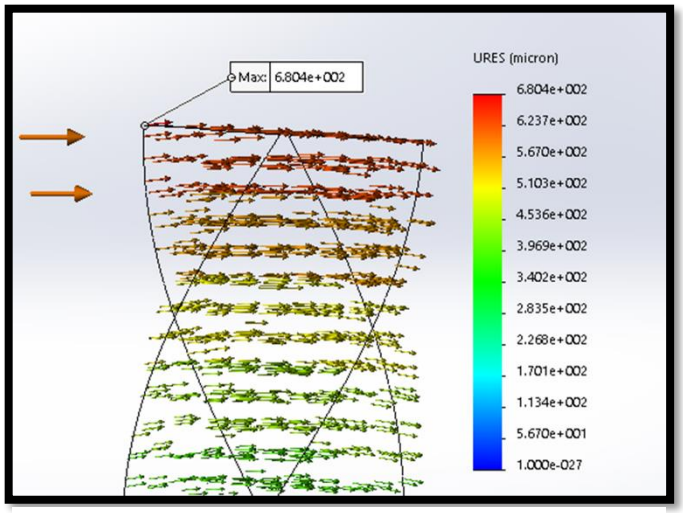

Figure 63 Vector plot of resultant displacement

Depth of Cut	Arbitrary Applied Force	Appropriated Force	Stress at Collet from Simulation	Appropriated Stress at Collet	Stress at Concentration from Simulation	Appropriated Stress at Concentration
30 Mils	500N	435N	3.75 GPa	3.26 GPa	5.60 GPa	4.87 GPa
15 MIls	250N	218N	1.90 GPa	1.65 GPa	2.80 GPa	2.44 GPa
2 MIls	33.3N	29N	250 MPa	218 MPa	390 MPa	339 GPa

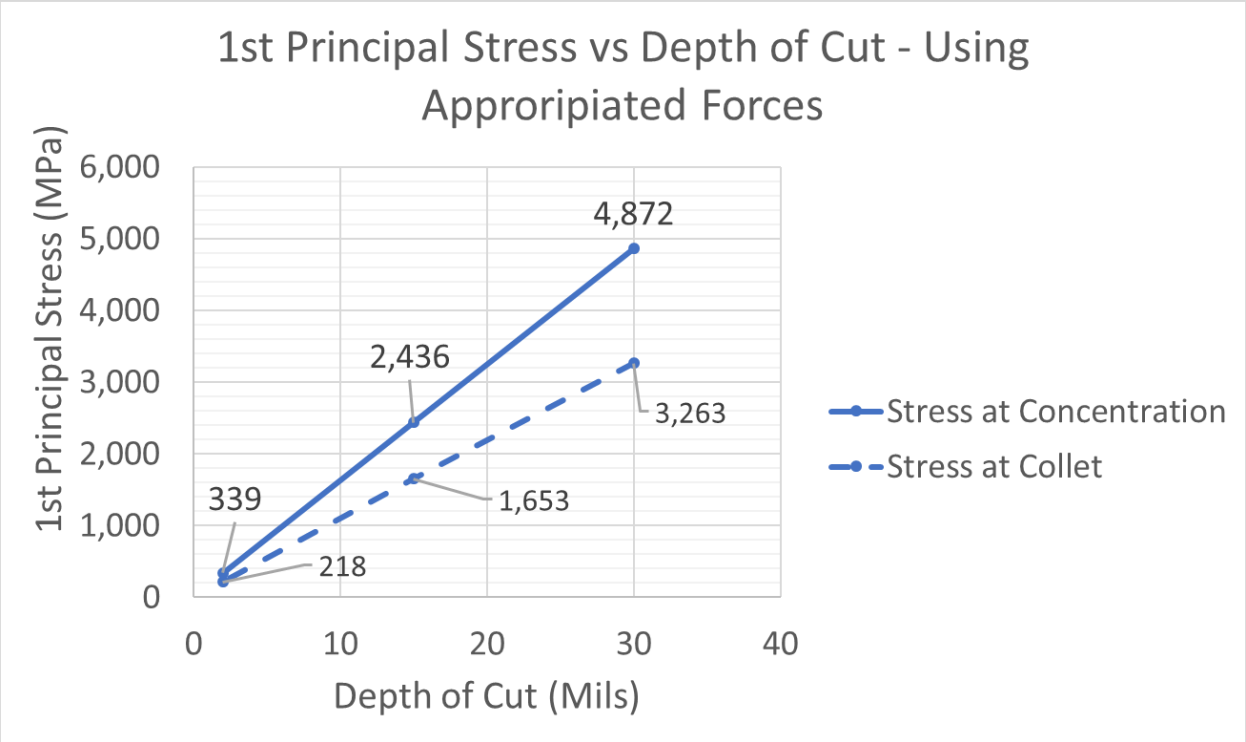

Figure 64

Discussion

Tungsten Carbide that is used to manufacture endmills, generally undergoes a heat treatment process that greatly increases the hardness of the material. Here we have assumed a value of 350 MPa which is a value for the material before any heat treatment, and therefore it is an under-estimation of tungsten carbide's ultimate tensile strength. We are then able to suggest cutting depths for safe operation so that the first principal stresses developed in the endmill would not exceed a value of 350 MPa. According to our data, the appropriated maximum stress for the 2-mil cutting depth is 339 MPa, located at the change in geometry between the flute and shaft.

Based on the results of our FEA studies and the extrapolation the studies allow us to do by the nature of SolidWorks Simulation as a linear solver, we are able to make the recommendation that the 1/8th inch diameter, four flute Tungsten Carbide flat end mill should only be used to make lateral cuts of depths of no more than 2 mils when cutting Chromoly Steel.

A cutting depth of 2 mils is very small, suggesting that the endmill studied should only be used, if at all, for finishing processes and tight geometries where no bigger tool could fit.

Conclusion

The direct conclusions drawn from the results of this project are limited in respect to the specific endmill used, the stock it was cutting, and the operational conditions of the milling machine. That is to say that the recommendation of performing lateral cuts safely at depths of 2 mils or less is only valid for the scenario which we have studied, an $1/8^{th}$ inch four flute, flat endmill cutting Chromoly Steel. Although limited, the direct conclusions were validated through experimental and analytical results, suggesting that a valid methodology has been developed for future work in static analyses of deflected endmills.

Common uses of FEA are to explore the redesign of parts and how they might perform, before having to physically manufacture the new design. This project only studied different cutting depths, an operational parameter, it did not explore any redesigns of the endmill itself; however, having established a validated solid modeling technique and finite element analysis procedure, the study of redesigning the part is quite feasible.

Possible redesigns of the four-flute flat endmill include but are not limited to: the number of flutes, the flute length, and the length of the smooth transition area between the flutes and the shaft. All the suggested possible redesigns can be easily studied by slightly altering some geometric parameters of the solid modeling process developed in this report. The redesigned model can then be studied using the same finite element analysis procedure developed in this report, to see how the stress distribution might develop. Then using the procedure developed here we can ensure that the stresses that develop do not exceed the ultimate tensile strength for the material that whatever end mill is in use, is made of.

References

[1] Kivanc, Evren Burcu, and Erhan Budak. "Development of Analytical Endmill Deflection and Dynamics Models." *Manufacturing | IMECE2003 | Proceedings | ASME DC*. American Society of Mechanical Engineers, 01 Jan. 2003. Web. 30 May 2017.

[2] "Tungsten Carbide Material Properties." *Tungsten Carbide, WC*. MatWeb, n.d. Web. 30 May 2017.

[3] DeGarmo, E. Paul, J. Temple. Black, and Ronald A. Kohser. *Materials and Processes in Manufacturing*. New York: Macmillan Pub., 1990. Print.